Analytical Methods

ROYAL SOCIETY OF CHEMISTRY

CRITICAL REVIEW

View Article Online
View Journal | View Issue

Cite this: *Anal. Methods*, 2024, **16**, 6771

Current trends in colorimetric biosensors using nanozymes for detecting biotoxins (bacterial food toxins, mycotoxins, and marine toxins)

Li Feng, * Mingcheng Zhang and Zhiyi Fan

Biotoxins, predominantly bacterial food toxins, mycotoxins, and marine toxins, have emerged as major threats in the fields of seafood, other foods, feeds, and medicine. They have potential teratogenic, mutagenic, and carcinogenic effects on humans, occasionally triggering high morbidity and mortality. One of the apparent concerns relates to the increasing consumption of fast food resulting in the demand for processed food without adequate consideration of the toxins they may contain. Therefore, developing improved methods for detecting biotoxins is of paramount significance. Nanozymes, a type of nanomaterials exhibiting enzyme-like activity, are increasingly being recognized as viable alternatives to natural enzymes owing to their benefits, such as customizable design, controlled catalytic performance, excellent biocompatibility, and superior stability. The remarkable catalytic activity of nanozymes has led to their broad utilization in the development of colorimetric biosensors. This has emerged as a potent and efficient approach for rapid detection, enabling the creation of innovative colorimetric sensing methodologies through the integration of nanozymes with colorimetric sensors. In this review, recent development in nanozyme research and their application in colorimetric biosensing of biotoxins are examined with an emphasis on their characteristics and performance. The study particularly focuses on the peroxidase (POD) activity, oxidase (OXD) activity, superoxide dismutase (SOD), and catalase (CAT) activity of nanozymes in colorimetric biosensors. Ultimately, the challenges and future prospects of these assays are explored.

Received 23rd June 2024
Accepted 28th August 2024

DOI: 10.1039/d4ay01184h

rsc.li/methods

1. Introduction

Nowadays, there is an emerging concern regarding the rapid monitoring of biotoxin presence in food products.[1,2] Biotoxins are frequently found in bacteria, viruses, fungi, protozoa, rickettsiae, and infectious substances polluting feed, food, condiments, seafood, and so forth. Biotoxins pose a risk to public health through the food chain by inducing both chronic and acute toxicity, as well as exhibiting carcinogenic, teratogenic, and mutagenic impacts on human health.[3–5] Certain biotoxin carriers and producers threaten human health and pollute the environment; they can lead to crop failures and diminish the quality of agricultural products. Marine toxins are categorized based on their carriers such as as ciguatoxins, shellfish toxins, mytilotoxin, tetrodotoxins, and others. There exists a wide range of marine toxins, exceeding 1000 different types, with several dozen having been effectively characterized. These toxins have the potential to infiltrate the food chain, leading to human toxicosis and potentially fatal outcomes. For instance, an estimated 750–7500 individuals die globally because of shellfish poisoning annually.[6] Bacterial toxins represent a distinct category of biotoxins capable of inducing foodborne illnesses through the inhibition of protein synthesis, leading to neurotoxic effects. The diseases are linked to the impact of bacterial toxins on tissues and are associated with distinct clinical symptoms. The most lethal bacterial toxin associated with food consumption is botulinum toxin, which is created by *Clostridium botulinum*. It has been reported that 100 ng of this toxin can be fatal to humans.[7] Mycotoxins are an important class of biotoxins that are produced as secondary metabolites by fungi, like *Fusarium*, *Aspergillus*, *Penicillium*, *Claviceps*, *Alternaria*, *Trichoderma*, *Stachybotrys*, *Verticimonosporium*, *Chaetomium*, and so forth, under favorable environmental conditions.[8] The contamination can happen throughout processing, harvesting, transportation, and storage. The International Agency for Cancer Research has classified mycotoxins into distinct categories according to their capacity to trigger cancer in humans. These classifications encompass Group 1, Group 2A, Group 2B, Group 3, and Group 4 carcinogens. For example, AFB1 (Group 1 carcinogen aflatoxin B1) is the most toxic and abundant group of mycotoxins. It has been shown to trigger lung carcinoma, hepatocellular carcinoma, colon carcinoma, and gallbladder carcinoma in humans. Liver cancer is caused *via* AFB1 in around 28.2% of individuals.[9]

Jiyang College, Zhejiang A&F University, Zhuji, Zhejiang 311800, China. E-mail: lifeng@zafu.edu.cn

In recent times, biosensors have emerged as a novel method of detection with a broad spectrum of applications for the timely quantitative/qualitative assessment of various biotoxins present in food products.[10] A biosensor is a diagnostic tool that integrates three components: a biorecognition unit (*e.g.*, aptamer, enzyme, antibody, phage, cell, *etc.*), a transducer and a signal conversion element.[11,12] The biorecognition unit is employed to specifically identify the target molecule. The interaction between the target molecule and the recognition unit initiates a series of physicochemical interactions. This reaction is characterized by changes such as light absorption and electrical signals, which form the basis for further signal transduction processes. The transducer, being the most crucial component of the biosensor, is capable of converting the above physicochemical alterations into quantifiable signals, thereby facilitating signal transduction. There exist various types of sensors that can be classified into four main groups based on distinct signal transduction methods: optical sensors, electrochemical sensors, magnetoelectric sensors, and piezoelectric sensors.[13,14] Among them, the optical sensor plays a crucial role in analyzing the optical signal produced during the integration of the target and the recognition unit, and then through the real-time conversion and signal amplification of the transducer, it will be converted into readable data to realize the quantitative sensing of the target substance. Colorimetric sensing technology is a quantitative optical method that relies on the correlation between the color change of a solution and the concentration of the target analyte. Compared with other optical sensors, the colorimetric sensor has the benefits of visualization, low cost, and simple operation, and could be coupled with a portable substrate, so the practical use is more extensive. This method provides naked-eye sensing abilities (qualitative) and could be incorporated with smartphone imaging (quantitative), making them well-suited for biotoxin presence detection in various foodstuffs.[15,16]

Enzymes are regarded as one of the earliest and most frequently utilized biometric components in biosensors. They have a dual role in recognizing the target substance and promoting electron transfer between the substrate, thereby catalyzing the chemical reaction of the specific substrate to induce corresponding signal alterations.[17] Enzymes have the capacity to act as indicators for the identification of particular substances, facilitating the transformation quantities of the target substance into detectable signals for analytical objectives.[18] As a result, the effectiveness of biosensor detection is somewhat dependent on the particular enzymes employed and their individual characteristics. The disadvantages of natural enzymes like difficulty in preservation, high cost, and poor stability limit their greater use in biosensors. The rapid advance of enzyme-like nanomaterials (also known as nanozymes) affords an innovative horizon for the choice of suitable signal markers for analyte identification. Nanozymes demonstrate catalytic properties like natural enzymes, allowing them to catalyze effectively even under extreme situations. This attribute expands the potential uses of nanozymes in biosensing applications.[19,20] The exceptional catalytic efficiency of nanozymes allows them to enhance the color change of platforms, resulting in the generation of light signals upon the colorimetric platform introduction. The colorimetric biosensor that utilizes nanozymes primarily depends on the catalytic capabilities of the nanozymes to imitate the natural enzymes' catalytic functions. This mechanism entails the conversion of a colorless substrate into a colored product through oxidation, enabling visual detection. In contrast to colorimetric biosensors lacking nanozymes, the integration of nanozymes with colorimetric biosensors could serve as a means of signal amplification to a certain extent, thereby enhancing the determination capabilities of biosensors.[21] Nanozymes have the potential to serve as recognition units for target analytes in biosensing systems, and their specific surface area offers more active sites to bind more targets, which could further enhance the sensitivity of colorimetric sensors. Furthermore, nanozymes do not possess inherent light-absorbing properties in colorimetric biosensors. However, upon the addition of a colorimetric substrate, nanozymes exhibit various mimetic enzyme activities that facilitate the catalysis of the substrate reaction, thereby initiating a light signal. This process contributes to signal amplification in colorimetric sensors.[22] Also, the surface properties and specific structures of nanozymes enable them to function as adsorbents for selectively adsorbing target molecules. This capability can enhance the selectivity of the colorimetric sensor.

By now, nanozyme-enabled colorimetric biosensors have been broadly employed in food safety analysis owing to the advantages of naked-eye visibility, high sensitivity, easy operation, and portability. However, the applications of nanozyme-enabled colorimetric biosensors in the field of biotoxin analysis have not been specially summarized. Therefore, in this review, we focus on the classification of nanozymes according to the different nanomaterials and offer a detailed description of each type of nanozyme. Moreover, we tried to discuss the construction approach of nanozymes in colorimetric biosensors in terms of catalytic activity, and afford a comprehensive review of the recent research progress of nanozymes in the colorimetric biosensing of various biotoxins (mycotoxins, marine toxins, and bacterial food toxins) in food products. Finally, the main challenges and prospects of nanozyme-enabled colorimetric biosensors are also deliberated.

2. Classification of nanozymes

Based on their functional activities, nanozymes can be classified into two primary groups: the oxidoreductase family and the hydrolase family. The oxidoreductases predominantly participate in redox reactions and exhibit various activities, including catalase (CAT), oxidase (OXD), superoxide dismutase (SOD), and peroxidase (POD) like functions. Hydrolases play a crucial role in catalyzing hydrolysis reactions and exhibit functions that are analogous to those of proteases, nucleases, phosphatases, *etc.*[23]. The constituents of nanozymes primarily consist of metals, metal oxides, sulfides, salts, metal–organic frameworks (MOFs), carbon materials, and metal–carbon hybrid nanocomposites.[24–26] Recently, studies on nanozymes have increasingly concentrated on nanomaterials that possess intrinsic catalytic properties, rather than enzymes or catalysts

immobilized on nanomaterials. Currently, the majority of published research regarding the classification of nanozymes has focused on categorizing them according to their catalytic activity. In order to offer further classification methods for nanozymes, this study concentrates on categorizing them using different nanomaterials and analyzes the fabrication approaches of colorimetric assays based on the various catalytic nanozyme activities.

2.1. Carbon-based nanozymes

Carbon-derived nanozymes, as a significant constituent of the nanozyme category, refer to carbon-based nanomaterials having enzyme-like catalytic functions. Owing to the benefits of environmental friendliness, low cost, good biocompatibility, and easy modification, carbon-based nanozymes are broadly employed in fields like biosensing, environmental protection, food safety, and disease diagnosis. Nevertheless, unlike other kinds of nanozymes, the synthesis of carbon-based nanozymes mainly relies on a trial-and-error approach. This methodology results in a notable level of uncontrollability in the modulation of the catalytic activity of carbon-based nanozymes. Furthermore, carbon-based nanozymes exhibit a lower degree of substrate specificity compared to other types of nanozymes, primarily due to the absence of substrate binding pockets. Consequently, there is a necessity to advance rational design approaches aimed at addressing this limitation. Extensive study into the characteristics of carbon-based nanomaterials has revealed their significant potential for uses related to catalytic features. The concept of carbon-based nanozymes was simultaneously introduced. The majority of carbon-based nanozymes are documented to exhibit POD-like or OXD-like function. Additionally, to enhance the catalytic properties of these carbon-based nanomaterials, the incorporation of other elemental dopants is often necessary. For instance, N-doped nanocarbon may show exceptional catalytic performance.[27] Nevertheless, the synthesis of N-doped carbon nanozymes with a high nitrogen content presents challenges due to the instability of the N element at high temperatures. In 2019, Wei and colleagues utilized polyethyleneimine (PEI) as a source of carbon and nitrogen, alongside montmorillonite (MMT) as a template, to synthesize a carbon-based nanozyme characterized by a high nitrogen content.[28] MMT was dispersed in an aqueous solution, after which the supernatant was subjected to incubation with a polyethyleneimine (PEI) solution. The obtained solution underwent freeze-drying to yield the assembled powder (MP), which was subsequently subjected to carbonization and etching processes to produce nitrogen-doped carbon nanomaterials. This study identified the critical factor, specifically the N doping content, which influences the catalytic performance of carbon-based nanozymes, and thus was of great importance for the development of carbon-based nanozymes with enhanced catalytic performance. Regardless of the significant progress, most of the existing carbon-based nanozymes exhibit only a singular enzymatic activity. Consequently, the development of methodologies to impart dual or multiple enzymatic activities to carbon-based nanozymes is of considerable interest. In light of this, Gao's team used Pluronic F127 as a soft template, and phenol, formalin and melamine as raw materials, to prepare a polymer, which consequently was pyrolyzed to acquire N-doped carbon.[29] The N-doped carbon N-PCNSs3, prepared under optimal conditions, demonstrated a porous nanosheet morphology, thus enabling the substrates to diffuse into the pores to increase reaction performance. Furthermore, the nitrogen content in N-PCNSs3 is significantly greater than that of other comparable materials, which enhances its multi-enzymatic activities and overall catalytic efficiency. As estimated, N-PCNSs3 had POD-, OXD-, SOD-, and CAT-like activities. It is evident that the catalytic function of carbon-based nanozymes depends on the precursor. Consequently, altering the precursor may represent a viable approach for the development of high-performance carbon-based nanozymes. In 2019, Choi and colleagues identified the photo-responsive glucose oxidase (GOx) and POD-like activities of carbon nitride by carbonizing melamine in the presence of KCl and KOH.[30]

Graphene, a subclass of carbon materials, features high conductivity, large surface area, strong thermal stability, and excellent transparency and thus, is considered a favorable candidate for preparing carbon-based nanozymes.[31] In 2015, Qu's team found POD-like activity in graphene quantum dots (GQDs) containing hydroxyl, carboxylic, and carbonyl elements, and thoroughly explored the catalytic mechanism. Following the activity test, it was determined that the carbonyl group serves as the active site and is responsible for determining catalytic activity. The carboxylic group interacts with the substrate, while the hydroxyl group does not.[32] To the best of our knowledge, this study explained the influence of surface functional elements on the catalytic functions of carbon-based nanozymes for the first time, and thereby will lead future researchers to progress the study of the preparation and design of high-performance carbon-based nanozymes. Nevertheless, graphene alone demonstrates minimal catalytic function. Graphene, in isolation, demonstrates minimal catalytic activity.[33] To enhance its activity, it is necessary to employ a doping strategy involving other elements such as N, P, B and S. Furthermore, it is essential to optimize the doping methodology to achieve the most effective coordination effects. In 2019, Lee and his colleagues introduced a series of N- and B-doped reduced graphene oxides, like BN-rGO, N-rGO, B-rGO (reaction between melamine and B-rGO), NB-rGO (reaction between H_3BO_3 and N-rGO), and h-BN-rGO (reaction between H_3BO_3, melamine, and rGO).[34] As expected, the synthesized rGO derivatives exhibited a nanosheet morphology, with the doped elements being uniformly distributed throughout the rGO matrix. This phenomenon may be attributed to the synergistic interaction between N and B, which notably enhanced the electron transmission rate during POD-assisted reactions.

2.2. Metal-based nanozymes

Metal-based nanozymes are one of the most typical nanozymes owing to their easy synthesis and stable structure. In general, metal-based nanozymes can be categorized into two primary

types: single-metal nanozymes and metal alloy nanozymes, which consist of multiple metal constituents. Furthermore, various metal-doped materials, including metal core/shell nanostructures, have been successfully synthesized.[35] These nanozymes show diverse shapes, like nanowires, nanoflowers, nanoparticles (NPs), nanosheets, and nanospheres. Various shapes can exhibit distinct catalytic characteristics. Among them, precious metal NPs like gold, silver, platinum, and palladium are commonly exploited in the determination of bacterial food toxins, mycotoxins, and marine toxins. The synthesis techniques of metal-based nanozymes comprise photochemical, high-temperature reduction, and mediated growth methods. In the experiments concerning nanozyme-assisted analyte sensing, the reduction technique is primarily utilized. For instance, PtNPs were produced using polyvinylpyrrolidone (PVP) as a stabilizing agent, and sodium citrate as a reducing agent, whereas AgNPs were prepared using potassium hydroxide and L-tyrosine as raw materials, which all have excellent peroxidase function.[36,37] In addition to exhibiting single-enzyme-like activity, certain metal-based nanozymes may also demonstrate multi-enzyme-like activity. For instance, peroxidase-like and oxidase-like Ir NPs were prepared based on PVP and $IrCl_3$–$3H_2O$ as raw materials through an alcohol reduction technique.[38,39] The combined influence of these two activities enhanced the sensitivity and selectivity of the nanozyme. Due to the synergistic interactions among each component, bimetallic nano-alloys frequently exhibit enhanced catalytic behavior. Recently, bimetallic nanocomposites received significant attention owing to their distinctive synergistic effect and multiple functions, and are extensively exploited in the catalytic field. The Au–Pt nanozyme demonstrated superior peroxidase-like activity compared to the Au nanozyme alone and exhibited greater stability over time than horseradish peroxidase (HRP). This phenomenon can be attributed to the disparity in electronegativity between Pt and Au, which facilitates the migration of electrons from Pt to Au. This transfer enhances the surface electron density of Au, thereby augmenting its catalytic activity.[40] To mitigate costs, copper (Cu) as an element was employed in the synthesis of bimetallic nanocomposites. Ramanathan *et al.* investigated the process of electroless deposition to facilitate the *in situ* growth of Cu NPs on the surface of cotton fabrics.[41] The obtained cotton fabrics were then submerged in an aqueous solution containing $AgNO_3$ or $HAuCl_4$ or $PdCl_2$ or H_2PtC_{l6} to prepare bimetallic nanoparticles, like Cu–Ag, Cu–Au, Cu–Pd or Cu–Pt. Cu–Pt NPs displayed excellent POD-like function and a remarkable catalytic rate. Despite the extensive research conducted on metal-based nanozymes, the tendency to aggregate and the toxicity associated with certain heavy metals pose significant limitations to their potential applications.[42]

2.3. Metal oxide-based nanozymes

Similar to metal-based nanozymes, recently, metal oxide/sulfide/salt-derived nanozymes have gathered considerable attention because they enjoy the merits of simple preparation steps, low cost, and distinctive magnetic/dielectric/optimal features.[43,44] Considering our understanding, the frequently applied techniques mainly include sol–gel, hydrothermal reaction, atomic layer deposition and air pyrolysis. Through adjusting the surface groups, structures, and categories, the catalytic behavior of nanozymes along with functionality and stability can be readily controlled. The pioneering research on nanozymes was documented *via* Yan in 2007. This study revealed that Fe_3O_4 NPs exhibited POD-like activity for the first time.[45] Employing TMB, OPD and diaminobenzidine (DAB) as substrates, Fe_3O_4 NPs catalyzed their oxidation producing blue, brown and orange colors, on the basis of which Fe_3O_4 NPs revealed POD-like function.

In addition to Fe_3O_4 NPs, V_2O_5 nanocomposites were also typically used to synthesize nanozymes, and to date, V_2O_5 enjoys OXD-, POD-, and dual-enzyme (GOx and POD)-like functions with 1D and 2D morphologies. The primary instance of V_2O_5 with POD-like performance was documented by Tremel's research team.[46] Initially, $KBrO_3$ and $VOSO_4$ were combined, after which HNO_3 was slowly added to achieve a pH of 2.0. Following this, thermal treatment was performed at 180 °C for 24 h to synthesize V_2O_5 nanocomposites. In another study, Doong *et al.* employed bulk V_2O_5 powder as the raw material, and used DMF to separate bulk V_2O_5 (ref. 47). The V_2O_5 nanosheets demonstrated significant oxidative activity, effectively catalyzing the oxidation of TMB to oxTMB. In 2023, Li *et al.* utilized the reaction between $KBrO_3$ and $VOSO_4$ to synthesize 2D V_2O_5 by optimizing the reaction conditions.[48] The resulting 2D V_2O_5 exhibited superior POD-like activity compared to V_2O_5 with other morphologies.

MnO_2 was also typically used to develop nanozymes with CAT-, POD-, OXD-, GOx- and SOD-like activities. For instance, Han and colleagues used BSA as a soft template to controllably produce a 2D MnO_2 nanozyme.[49] Actually BSA with rich NH_2 and –COOH groups could efficiently fix Mn^{2+} in its molecular structure to generate Mn^{2+}@BSA. Upon the addition of NaOH, Mn^{2+} present in the Mn^{2+}@BSA complex was initially converted into MnO(OH). This intermediate subsequently underwent oxidation by O_2, ultimately resulting in the formation of MnO_2. As anticipated, the synthesized MnO_2 under alternative conditions exhibited an irregular flocculent morphology, highlighting the significant influence of BSA.

To sum up, metal oxide-based nanozymes, such as peroxidase-like V_2O_5, GeO_2, TiO_2, Fe_3O_4, and oxidase-like MnO_2, are also employed in the determination of various toxins. Nevertheless, unmodified metal oxide-derived nanozymes might display poor stability and other challenges.[50] Consequently, further research is needed to alter specific components within the metal oxide to enhance its detection efficacy.

2.4. MOF-based nanozymes

MOFs are crystalline materials characterized by a periodic network structure that arises from the self-assembly of organic components, typically organic ligands such as pyridine or carboxylic acids, in conjunction with metal clusters or metal ions, predominantly comprising transition metal ions like Fe^{2+}, Zn^{2+}, and Cu^{2+}.[51,52] MOFs are a class of nanomaterials that have

garnered significant interest in recent years due to their advantageous characteristics, including a high specific surface area, a porous network structure, and tunable chemical properties.[53] Poor selectivity is prevalent among numerous nanozymes; therefore, it is essential to conduct a thorough investigation into the factors contributing to the high selectivity observed in natural enzymes and to incorporate these insights into the development of nanozymes. Similarly, when utilizing MOF-based nanozymes *in vivo*, it is imperative to assess their cytotoxicity and biosafety to confirm that they do not pose any harm to the organism. According to their synthesis approaches, MOF-based nanozymes can be divided into chemically modified MOFs, pristine MOFs, MOF derivatives and MOF-based composites.[54]

The coordination binding sites of the metal centers within MOFs are often obstructed by the organic moieties, leading to diminished catalytic activity. Therefore, it is imperative to explore novel strategies to address this issue and enhance the catalytic performance of the unmodified MOFs. Strategies have been established to augment their catalytic performance, like assembly of metal nanoparticles, surface modification of MOFs, metal oxides, and other constituents in MOFs.[55] Fe_3O_4@MIL-100(Fe) composites were effectively synthesized using an *in situ* growth technique, which involved the incorporation of Fe_3O_4 NPs within the MIL-100 framework. The catalytic potential of these MOF composites for photo-Fenton reactions was subsequently investigated.[56] Research has also been conducted on the synthesis of AuNPs@MIL-101 composites through the hydrothermal deposition of AuNPs onto the MIL-101 MOF. This composite material exhibits catalytic properties for the oxidation of ascorbic acid, which can be utilized in conjunction with an electrochemical sensor for the detection of microcystin-LR in water samples.[57] Both rGO and TiO_2 have been revealed to couple with MIL MOFs to improve their catalytic function.[58,59] In addition, MOFs could also be applied as templates or precursors to provide a series of MOF derivatives, for example carbon materials, metal oxides, metals, and so on, owing to their modifiable structures. For instance, by calcining the precursors of Fe-ZIF-67 and Fe-ZIF-8 at high temperatures, an Fe–N–C nanozyme with POD-like function was achieved, which exhibited good performance.[60]

3. Colorimetric biosensors using nanozyme activity

As is well known, colorimetric biosensing relies on the correlation between the extent of color alteration in the platform and the concentration of the analyte substance to enable quantitative determination. The alteration in substrate color is dependent on the catalytic function of the enzyme. Nanozymes typically facilitate the conversion of a colorless substrate into a colored one through their inherent enzyme-like properties. For instance, nanozymes exhibit the ability to induce color changes in various substrates, including OPD (*o*-phenylenediamine), TMB, ABTS, and other chromogenic substrates, enabling colorimetric recognition. Recently, most of the research endeavors concerning the catalytic capabilities of nanozymes have primarily concentrated on imitating oxidoreductase characteristics, specifically those associated with OXD, POD, CAT, and SOD functionalities.[61] Some previous studies have explored hydrolytic enzyme mimics, however, the focus has shifted towards the oxidoreductase-imitating capabilities of nanozymes, particularly in the context of colorimetric sensing. This section primarily examines the development strategies and advancements in the employment of colorimetric nanoprobes that leverage the oxidoreductase-like properties of nanozymes. In recent years, there has been a growing interest in the integration of biosensors with innovative nanomaterials, and nanozymes are broadly exploited in colorimetric recognizing platforms owing to their superior stability and exceptional catalytic characteristics. From one perspective, nanozymes have the potential to serve as biorecognition units for analytes in biosensing applications, as they offer a large specific surface area that can render numerous active sites for binding multiple targets, which in turn can effectively boost the sensitivity of colorimetric sensors.[62,63] Furthermore, nanozymes lack inherent light-absorbing characteristics in colorimetric nanoprobes. However, upon the addition of a colorimetric platform, nanozymes exhibit diverse simulated enzyme performances that facilitate the catalysis of the surface reaction, thereby initiating a light signal. This mechanism enables nanozymes to contribute to signal enhancement within colorimetric probes.[22] Additionally, the distinct structure and interface characteristics of the nanozymes enable them to function as adsorbents for selectively capturing the desired molecules. This capability could enhance the colorimetric assay selectivity. More importantly, nanozymes play a crucial role in inducing a color change in the substrate as part of the catalytic process. This transformation enables the conversion of the concentration or amount of the desired molecules into visible hue indicators, facilitating the naked eye detection of signal variations through colorimetric sensors.

3.1. POD-like activity

Peroxidase could catalyze reactions in the presence of peroxides such as ROOH, acting as a H_2O_2 redox substrate and electron acceptor, converting them into oxidation products and H_2O products.[64] The nanozymes' POD mimetic system exhibits a ping-pong mechanism and Michaelis–Menten kinetics similar to those observed in the catalytic behavior of natural peroxidase enzymes.[61] The ping-pong mechanism is defined by the enzyme's alternating transition between its initial conformation and an altered state. This process involves the enzyme releasing the initial product upon binding with the initial substrate in its base state, transitioning to the altered form, and reverting to the original conformation upon binding with the second substrate to release the subsequent product.[65] In contrast to the OXD mimetic activity, the POD mimetic system requires the presence of H_2O_2. H_2O_2 serves as a natural scaffold toward POD, and the nanozymes facilitate the breakdown of the O–O bond in H_2O_2 into $^{\bullet}OH$ with a significant oxidation potential. The resulting $^{\bullet}OH$ species can subsequently oxidize various colorimetric

substrates, including OPD, ABTS, TMB, and other similar compounds.[22] The production of $^{\bullet}OH$ in processes mimicking peroxidase enzyme activity has been documented through two pathways. One pathway involves the Fenton reaction, where Fe^{2+} reacts with H_2O_2 to produce $^{\bullet}OH$ and hydroxides (OH^-). The Haber–Weiss reaction as a second pathway can catalyze superoxide ($^{\bullet}O^{2-}$) *via* iron ions and H_2O_2 leading to the generation of $^{\bullet}OH$.[66]

The emerging trend in analytical chemistry involves utilizing nanozymes with inherent peroxidase-like activity in conjunction with colorimetric biosensors for the purpose of detecting specific target substances. This approach uses the catalytic color development concept through nanozymes. Graphite-like carbon nitride (g-C_3N_4) nanosheets exhibit properties similar to POD enzymes with notable stability. Notably, the functionalization of g-C_3N_4 with heteroatoms has been shown to substantially improve its POD-like activity. In this regard, Fu's group activated g-C_3N_4 with Pd NPs for the improvement of its enzyme-catalyzed performance and loaded the heteroatom-activated g-C_3N_4 with Fe_3O_4.[67] A magnetic platform consisting of Fe_3O_4/Pd NPs supported on g-C_3N_4 was developed to enhance POD-like activity and utilized for immobilizing different natural enzymes, aiming to achieve material reusability and mitigate optical nanozyme interference caused by scattering in colorimetric sensors. Using Fe_3O_4/Pd NPs/g-C_3N_4/GOx, a colorimetric probe was developed for the determination of glucose. There was no detectable evidence at 652 nm when TMB, glucose, and Fe_3O_4/Pd NPs/g-C_3N_4 without GOx were present, indicating that Fe_3O_4/Pd NPs/g-C_3N_4 does not exhibit an inherent GOx-like function. The alteration in TMB hue was observed only when Fe_3O_4/Pd NPs/g-C_3N_4/GOx, TMB, and the target were co-present.

In another study, Li *et al.*[68] produced S- and N-doped carbon-loaded POD-like FeCoZn triatomic catalysts that stemmed from ZIF-8 by taking benefit of two properties, specifically, the efficiency of MOFs in mitigating the issue of single-atom catalyst agglomeration and the potential of dispersing multiple metal atoms to boost the efficiency of single-atom nanozymes. A colorimetric nanozyme using a dual-channel assay was developed by integrating FeCoZn-TAC/SNC with a sensor array, aimed at differentiating food preservatives (Fig. 1). The FeCoZn-TAC/SNC nanozymes exhibit POD-like activity, facilitating the color development reactions of TMB and OPD to yield green and yellow products, respectively. The food preservatives can adhere to the nanozyme surface *via* hydrogen bonding and π–π stacking interactions. The diverse levels of interaction noted between FeCoZn-TAC/SNC and different food preservatives led to a reduction in the catalytic efficiency of the nanozymes. Consequently, this occurrence resulted in varying degrees of color signals, which serves as the fundamental mechanism for discriminating the preservatives. According to this principle, the colorimetric reaction profiles of various preservatives exhibit variations. Through linear discriminant analysis, a 100% accuracy rate was attained during the cross-validation of seven food preservatives. This result indicates that the sensor array adeptly distinguished seven varieties of food preservatives even at low concentrations.

3.2. Oxidase-like activity

Oxidases have the ability to facilitate the oxidation of substrates (such as electron donors) in the presence of molecular oxygen or other oxidants (such as electron acceptors), leading to the formation of oxidation products along with H_2O, H_2O_2, or O^{2-}.

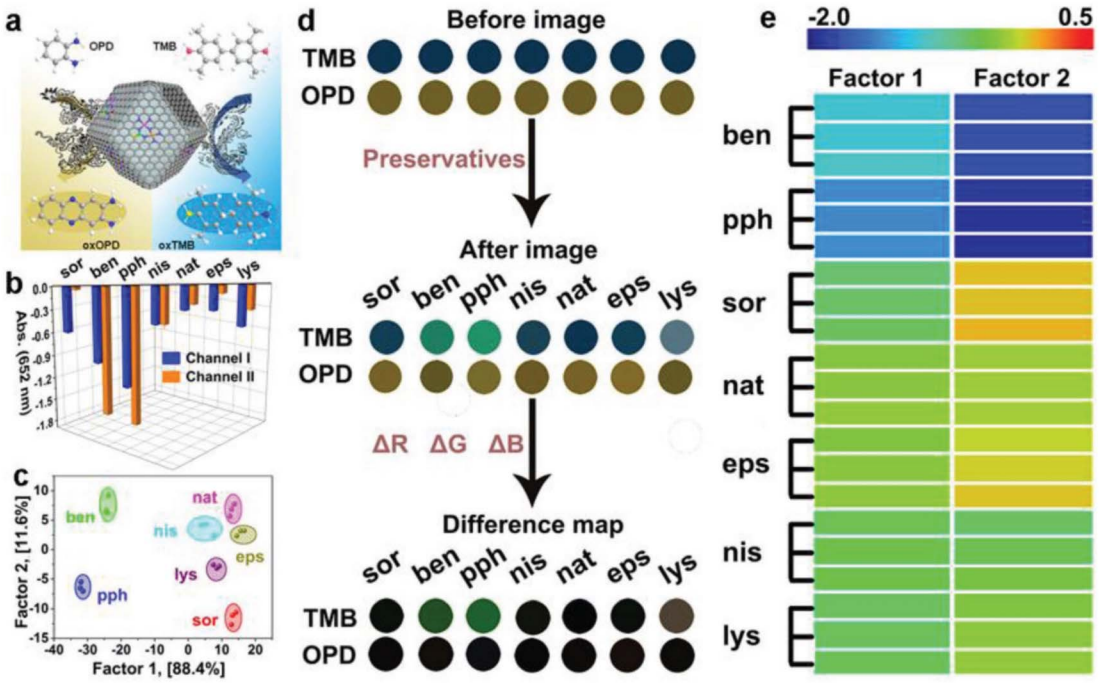

Fig. 1 Schematic drawing of the fabrication of a colorimetric biosensor using a two-channel array on the basis of the POD-like function of nanozymes for discriminating food preservatives. Reprinted with permission from ref. 68.

Currently, a variety of nanozymes have been identified to exhibit oxidase-like activity. Massimiliano and colleagues discovered that gold nanoparticles (Au NPs), even when not loaded with protective agents, exhibited enhanced catalytic activity. Bare Au NPs exhibited the ability to catalyze the production of H_2O_2 and gluconate from glucose in the presence of O_2. In contrast, colloidal particles of Ag, Cu, Pt, and Pd did not demonstrate comparable activity under identical conditions.[69] Thereafter covalent organic frameworks, metal–organic frameworks, carbon-derived nanozymes, and other nanozymes have been identified to possess OXD-like activity.[70–73] Colorimetric biosensors can be developed by utilizing the color change resulting from the catalytic activity of oxidases, where the *in situ* production of superoxide radicals and hydrogen peroxide oxidizes colorless substrates into colored products.[74] To some extent, the OXD mimics are considered more appropriate for biochemical analysis compared to the POD mimics due to their ability to function without the need for H_2O_2 in the catalytic procedure. Additionally, the reaction conditions for the enzyme mimics are simpler and more direct. Nevertheless, Singh and colleagues found that nanozymes possessing OXD-like activity have the capability to trigger molecular oxygen conversion into reactive oxygen species like singlet oxygen, oxygen radicals, and hydroxyl radicals during the catalytic mechanism, which can be effectively utilized for the oxidation of diverse substrates.[75–77] This results in a lack of specificity in the catalytic activity of the nanozymes. In order to address this issue, they developed a biomimetic approach utilizing MOF materials. Through the manipulation of MOF crystal growth in the *Z* direction, researchers successfully synthesized ultrathin nanosheets of Mn-UMOF using benzene dicarboxylic acid and triethylamine. The presence of the robust donor ligand triethylamine and the bridging ligand benzene dicarboxylic acid in Mn-UMOF leads to an increased density of active sites and enhanced substrate binding properties, especially for the case of electron unsaturation, when compared to the bulk Mn-BMOF. Additionally, Mn-UMOF could better catalyze the oxidation of substrates such as amplex red (AR), ABTS, and TMB without any external oxide addition.[78]

In another study, Zhang's team established an innovative technique that can selectively identify thiophanate-methyl.[79] A Cu-doped carbon nanozyme, denoted as Cu@NC, was

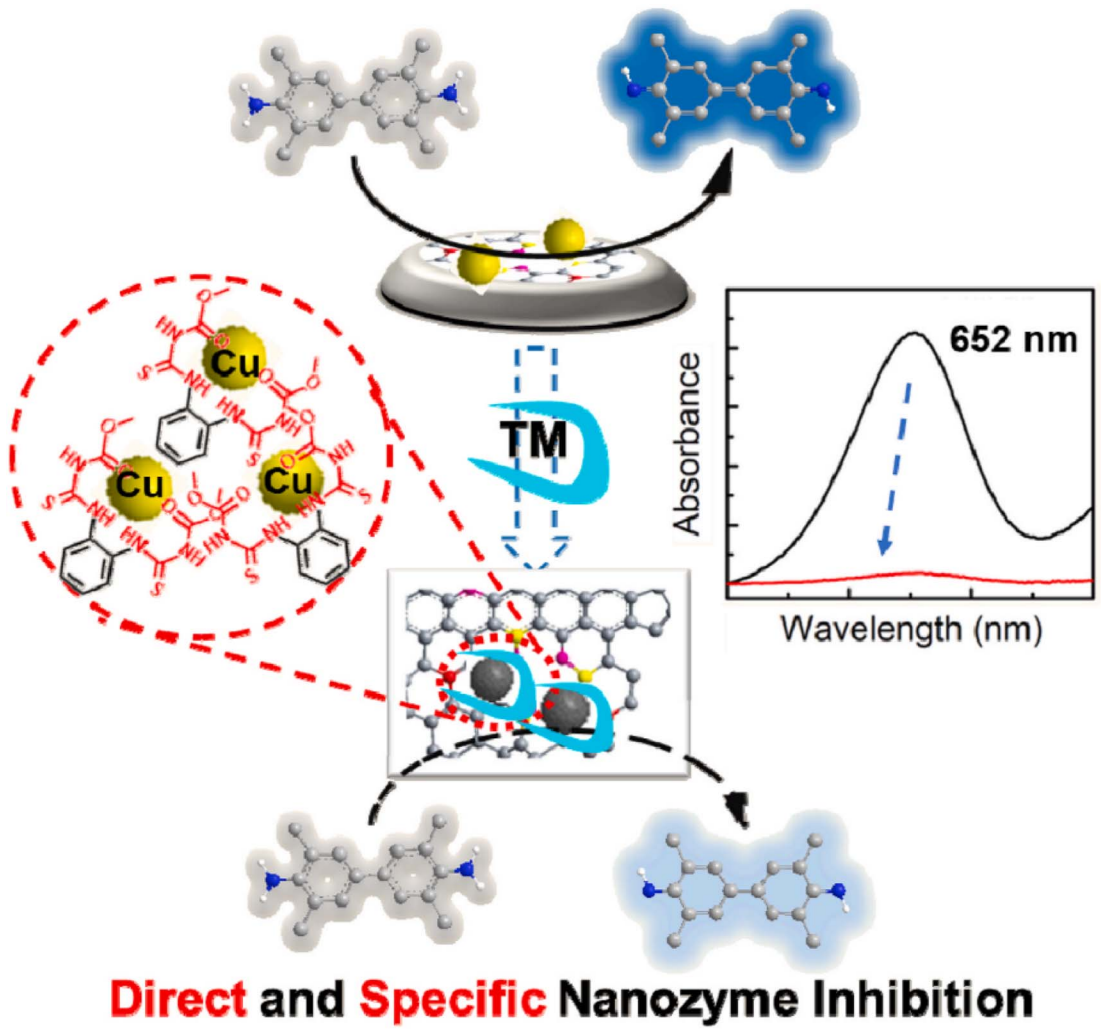

Fig. 2 Diagram illustrating the development of a colorimetric nanoprobe utilizing the OXD-like properties of nanozymes for the precise identification of thiophanate-methyl. Reprinted with permission from ref. 79.

developed with Cu serving as the active center site. The thiocarbamide-like and ethylenediamine-like building blocks in the target analyte, thiophanate-methyl, exhibit a robust affinity for metal ions. This property enables thiophanate-methyl to selectively interact with Cu@NC in the presence of other pesticides, leading to a significant reduction in the catalytic performance of the nanozyme and facilitating colorimetric detection (Fig. 2). The researchers also examined the specificity of the colorimetric sensor and revealed that thiophanate-methyl had a direct and specific inhibitory effect on the OXD performance of Cu@NC nanozymes. To examine the mechanism through which the nanozyme activity is inhibited, experiments were carried out. These experiments revealed a reduction in the nanozyme catalytic activity after pre-incubating the target molecule, thiophanate-methyl, with Cu@NC. Subsequently, thiophanate-methyl was introduced to the chromogenic substrate. Upon the introduction of thiophanate-methyl into the conventional system consisting of TMB and Cu@NC, it was observed that the catalytic activity remained unaffected. This suggests that the decrease in Cu@NC activity caused by thiophanate-methyl is a result of its direct interaction with Cu@NC, rather than from enhancing the reduction of oxTMB. Additional inhibitory elements were subsequently examined, and it was finally found that TM can be fixed onto the Cu@NC interface *via*

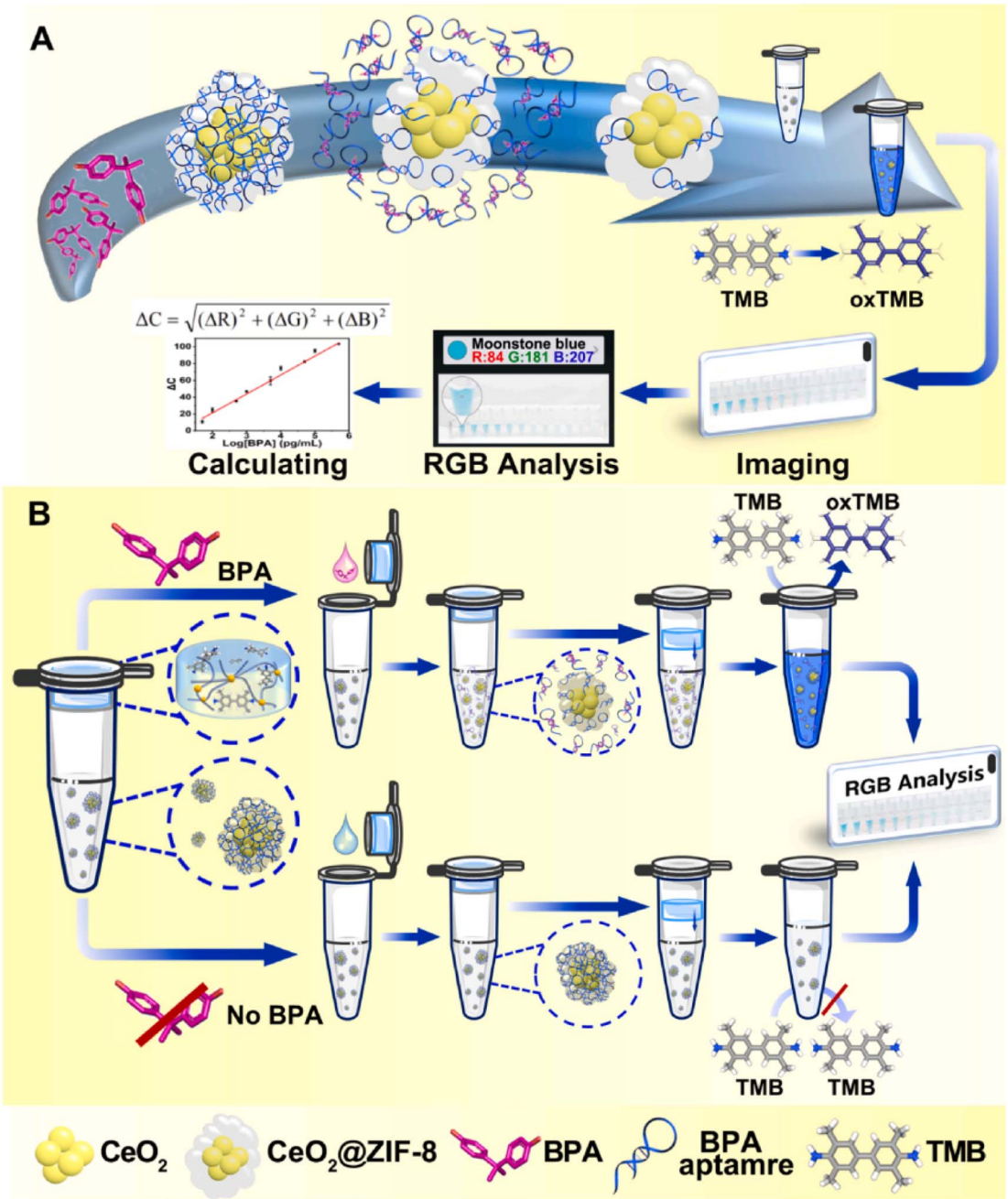

Fig. 3 (A) Diagramatic description of the fabrication and the OXD-like properties of CeO_2@ZIF-8/Apt nanoprobes. (B) The sensing mechanism of a one-pot portable testing substrate for bisphenol A determination. Reprinted with permission from ref. 80.

π–π stacking interactions and attached to its metal sites to suppress its catalytic function.

CeO_2 nanoparticles demonstrate remarkable mimetic activity similar to oxidase enzymes, enabling the catalysis of TMB color progress in the absence of hydrogen peroxide. In this regard, Jia's group developed a multifunctional portable colorimetric detecting substrate for the determination of bisphenol A.[80] As depicted in Fig. 3, the experimental configuration utilized the CeO_2@ZIF-8/Apt nanoprobe as both the signal generation unit and recognition component. Sodium alginate hydrogel tubes were employed to contain the TMB and catalytic reaction buffer as the reaction medium. The hydrogel containing the TMB platform was attached to the top of the tube, while the signal probe was placed at the base of the tube. Following the introduction of the sample and subsequent mixing with the signal probe, the Apt molecules on the signal probe dissociated and attached to the target, which resulted in the triggering of the OXD activity of the CeO_2@ZIF-8. Upon completion of the reaction process, photographs of the reaction solution were taken using a smartphone, and were subsequently uploaded to a color analyzer based on the RGB app. This method was employed to quantitatively evaluate the target object.

3.3. Catalase-like activity

The catalase enzyme facilitates the degradation of hydrogen peroxide into oxygen and water. The catalase-like properties of NPs were first reported in amine-terminated PAMAM dendrimers that encapsulated gold nanoclusters, which were observed under both physiological and acidic conditions.[81] Likewise, several compounds with a nanozyme-like activity such as manganese oxide (Mn_3O_4) nanoparticles, platinum nanoparticles, and cerium oxide nanoparticles are designed to display a catalase-like activity. The molecular-level investigation of the catalase-like behavior of nanozymes explores mechanisms involving bi-hydrogen peroxide association, base-like dissociation, or acid-like dissociation.[82] The bi-hydrogen peroxide mechanism has been identified as the most appropriate explanation for the catalase-like activity in nanozymes, particularly in the case of cobalt (II, III) oxide (Co_3O_4) nanoparticles. The catalase-like activity of cerium oxide nanoparticles involves the oxidation of hydrogen peroxide on the nanoparticles' surface to form oxygen. This process leads to the reduction of cerium oxide to H_2-ceric oxide. Subsequently, H_2-ceric oxide reacts with another hydrogen peroxide molecule, resulting in the production of water.[83] Furthermore, Zhang *et al.* illustrated the catalase-like function of iron-based single atom nanozymes (Fe-SANzymes) *via* obviously exposed edge-hosted defective Fe/N_4 atomic sites.[84] The mechanistic investigation demonstrates that defects facilitate a substantial charge transfer from the Fe atom to the carbon matrix. This process activates the central Fe atom, enhancing its interaction with hydrogen peroxide and simultaneously weakening the O=O bond.

3.4. Multi-enzyme-like activity

Nanozymes with a CAT-like function are frequently employed to eliminate the extra-naturally occurring reactive oxygen hydrogen peroxide, which is somewhat close to POD enzymes. Nevertheless, nanozymes typically lack the ability to oxidize substrates to enhance hue. Consequently, it is less frequent to depend solely on nanozymes in terms of the CAT activity for the fabrication of colorimetric nanoprobes. Superoxide dismutase is a metalloenzyme with antioxidant properties found in various organisms, capable of enabling the dismutation of reactive superoxide anion radicals into O_2 and H_2O_2. SOD enzymes like CAT enzymes were frequently employed to neutralize surplus reactive oxygen classes, playing a pivotal role in the body's oxidation and antioxidant equilibrium. The catalytic mechanism of SOD enzymes primarily entails the protonation of a superoxide anion ($O_2^{\bullet -}$), which is in turn protonated by water to produce OH^- and $HO_2^{\bullet}$ radicals. Nanozymes with $O_2^{\bullet -}$ scavenging ability are considered to be favorable substitutes to natural SOD enzymes. If nanozymes demonstrate multiple simulated enzyme functions simultaneously, like SOD, OXD, and POD, the dominant activity is expected to be the SOD enzyme activity. This activity is influenced by factors like environmental pH, surface ions, and nanomaterial structure.[85] Currently, the majority of reported nanozyme activities focus on POD and OXD activities, with limited research on mimicking SOD activity. Moreover, given that the primary purpose of the SOD enzyme is to preserve redox equilibrium in cells and mitigate oxidative stress, a significant portion of research endeavors focusing on nanozymes with SOD-mimetic characteristics are primarily directed towards mitigating inflammation. In contrast, there is a conspicuous lack of research investigating the employment of SOD nanozymes in colorimetric recognizing methodologies. Like CAT enzymes, the utilization of SOD-like nanozymes in colorimetric probes typically depends on the multifunctional enzyme properties of the nanozymes.

4. Applications of nanozymes based on the colorimetric biosensor for biotoxin detection

4.1. Mycotoxin detection

Mycotoxins, as one of the most alarming food and feed contaminants, are carcinogenic and highly toxic secondary metabolites produced by specific fungi, predominantly molds, which have the potential to contaminate a broad spectrum of crops (including nuts, grains, and legumes) and this, in turn, can be transferred to various food products. These naturally occurring toxins pose a substantial risk to humans, with exposure capable of inducing numerous adverse effects such as acute poisoning, chronic ailments, and potentially cancerous consequences. Mycotoxins are typically prevalent in cereals, grains, nuts, spices, coffee, cocoa, dried fruits, and animal-sourced products such as milk and meat. Prominent and extensively researched mycotoxins comprise aflatoxins, ochratoxins, fumonisins, trichothecenes, and zearalenone.[86,87] Therefore, the implementation of effective and innovate mycotoxin analytical detection methods, and alongside that, novel nanomaterials, has become pivotal for safeguarding humans

against health dangers and risks. This section has been conducted to review the detection of major mycotoxins, including aflatoxin B_1 (AFB1) and ochratoxin A (OTA), based on nanozymes.

4.1.1. Aflatoxin. Aflatoxins are hazardous secondary metabolites primarily synthesized by *Aspergillus* fungi. These toxins reveal significant mutagenic, carcinogenic, and teratogenic potency in both human and animal subjects. Corn, rice, peanuts, dried fruits, spices, and dairy products can be considered the most important sources of these toxins. Among different aflatoxins, AFB_1 is the most dangerous member of the aflatoxin group, as a Group 1 carcinogen, responsible for the majority of all aflatoxin-associated feed and food contamination.[88,89] In this regard, the maximum allowable limit of AFB_1 in foodstuffs was set at 1.0–20 μg kg^{-1}. The field of biosensors based on various nanozymes including single-atomic nanozymes,[90] MOFs,[55] and metal nanoparticles[19] is rapidly evolving, with ongoing research focused on understanding their mechanisms of action and increasing their catalytic efficiency. In favor of the application of metal nanoparticles as nanozymes, two metal components demonstrate better peroxidase catalytic performance than monometallic nanozymes. For example, Zhao *et al.*[91] reported a surface-enhanced Raman scattering (SERS) sensor based on gold–mercury nanoparticles (Au@HgNPs) coupled with carbon dots (CDs) for AFB_1 determination. In this study, the poor colloidal stability and low enzyme-like activity of the AuNPs were distinctly improved by using Hg^{2+}. This modification could be beneficial for the oxidase-mimicking activity of the AuNPs, attributed to the reduction of Hg^{2+} to metallic Hg^0 forming Au@HgNPs. Under optimal conditions, the presence of the target inhibited the aggregation of Au@HgNPs, through oxygen atoms in the carbonyl group, which enhanced SERS signal intensity. In 2022, Lai *et al.*[92] focused on introducing a simple and rapid synthesis method of nanozymes by simply mixing Cu(II) and $K_3[Fe(CN)_6]$ for producing copper hexacyanoferrate nanoparticles (CHNPs) for the purpose of AFB_1 detection. Elaborately, in contrast to the common nanozyme synthesis methods which rely on re-synthesized nanomaterials, the nanozyme was designed in this biosensing platform without requiring the tedious process and preparation of nanomaterials. Therefore, this biosensing approach can broaden our horizon on another important factor in terms of the application of nanozymes in toxin detection, which is tedious nanozyme preparation, by offering a simple, rapid, and accessible way to generate the nanozyme on-demand. Interestingly, bimetal nanozymes demonstrate better catalytic efficacy compared to their single-metal counterparts, owing to the synergistic interplay between the two metal varieties. Most recently, Wu and co-workers[93] exploited mesoporous SiO_2/gold–platinum (Au–Pt), m-SAP, in the structure of a colorimetric biosensing device for AFB_1 detection. In this protocol, mesoporous SiO_2 nanospheres were loaded with Au–Pt, achieving high catalase like activity. In the absence of the target, the complementary DNA conjugated m-SAP was captured by

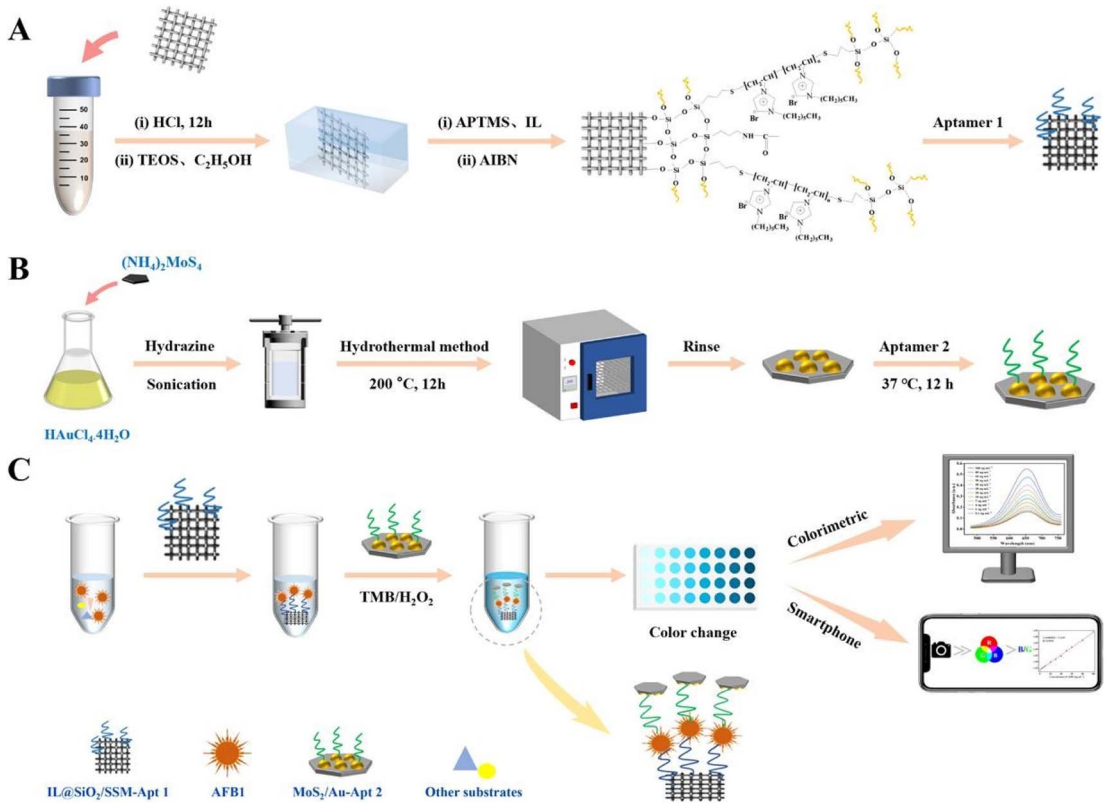

Fig. 4 (A–C) Representation of the colorimetric aptasensor based on MoS_2/Au for AFB_1 determination. Reproduced with permission from ref. 94 Copyright Elsevier Science, 2024.

aptamer-magnetic nanoparticles and facilitated the formation of 3,3′,5,5′-tetramethylbenzidine (TMB)/H_2O_2 coloring system. The detection limit of the developed colorimetric aptassay was 5 pg mL^{-1}, 600-fold lower than that of traditional ELISA. In addition, during interference testing, AFB_1 could be differentiated from six other interfering substances. In order to achieve a more reliable and highly sensitive nanozyme based on two metal varieties, Jiang and colleagues[94] exploited the advantages of a bimetallic MoS_2/Au nanozyme, as a substrate for immobilization of aptamers, in developing a sandwich-based colorimetric aptasensor of AFB_1 (Fig. 4). In this work, the synergic effect between MoS_2 and Au increased the catalytic activity and stability. In detail, the low Michaelis constant (K_m) and the high maximum reaction rate (V_{max}) of MoS_2/Au in comparison to single-component MoS_2 or Au nanomaterials demonstrated the stronger binding affinity and superior catalytic efficiency, respectively. Importantly, the specific structure, the flower-like MoS_2/Au composite, introduced numerous surface-active sites through its unique multilayered and porous structure which was considered an excellent immobilization substrate of aptamers. Furthermore, the high surface area and porous structured silica aerogel modified stainless-steel mesh (SiO_2/SSM) could immobilize the negatively charged aptamer2. Under normal circumstances, the construction of the sandwich aptassay was conducted by capturing AFB1 *via* SiO_2/SSM, followed by binding of the MoS_2/Au/aptamer1. This structure was successfully employed to quantify AFB_1 in different real food samples including peanut, corn, and wheat, with negligible matrix effects (90.84–106.11%) and recoveries of 88.52–113.40%.

Another excellent example of this concept was implemented in a colorimetric and photothermal dual-mode immunoassay using the peroxidase-like activity of Pt supported on nitrogen-doped carbon for AFB_1 quantification.[95] As shown in Fig. 5, glucose oxidase (GOx)-labeled AFB_1-bovine serum albumin (BSA) competes immuno-competitively with AFB_1, thereby releasing GOx to catalyze the glucose production of H_2O_2. Under normal conditions, the colorimetric signal was produced due to the oxidation of TMB to TMB_{Ox}. Along with the colorimetric signal, a thermal signal was achieved when TMB_{Ox} underwent photothermal conversion under 808 nm laser irradiation. The fabricated biosensor was able to detect AFB_1 with an LOD of 0.22 and 0.76 pg mL^{-1}.

The application of multimodal biosensors based on nanozymes in AFB_1 determination can introduce different signals, extending the linear range of quantification. In addition, these signals can be mutually verified to improve the accuracy of biosensing approaches.[96,97] Another dual-mode approach for AFB_1 quantification based on the Ag@Au IP6 bifunctional nanozyme, with peroxidase-like activity and SERS effect, was reported by Tan and colleagues.[98] For this purpose, the surface of magnetic particles was decorated with AFB_1 aptamers along with a trigger probe. In the presence of the target, the conjugation of targets with specific aptamers led to the trigger probe and this, in turn, initiated a hybridization chain reaction (HCR) which introduced alkaline phosphatase (ALP), catalyzing the self-assembly of the Ag@Au IP6 nanozyme. The constructed nanozyme revealed increased peroxidase-like activity, improving the oxidation of TMB to the blue-colored TMB_{Ox}; additionally, its core–shell

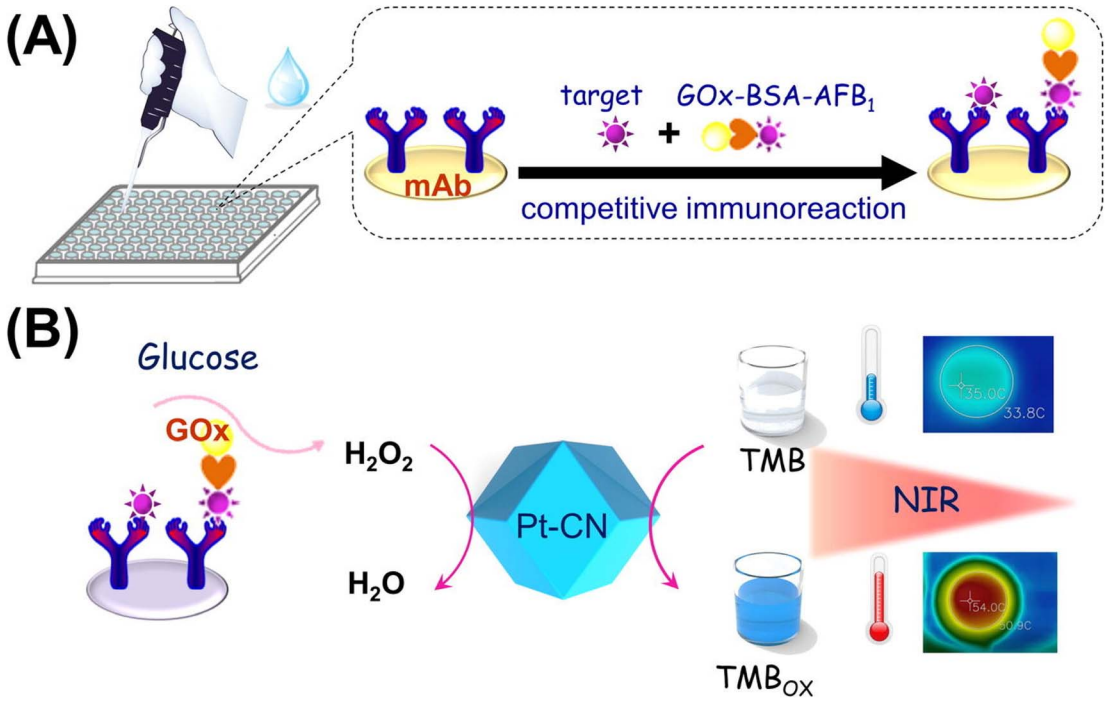

Fig. 5 (A) Competitive immunosensor exploiting the GOx-labeled AFB_1-BSA conjugate as the tag. (B) Illustration of colorimetric and photothermal measurement based on H_2O_2-responsive peroxidase-like activity of Pt–CN. Reproduced with permission from ref. 95. Copyright Elsevier Science, 2019.

structure also enabled strong SERS enhancement of the TMB_{Ox} signal.

Particularly, from an economic perspective, substituting precious metals that contribute to the activity of nanozymes, with more affordable transition metals, in the structure of nanozymes can markedly reduce the expenditure associated with nanozymes. For instance, Cai *et al.*[99] designed a novel colorimetric nanozyme-based lateral flow assay (LFA) based on MnO_2 nanosheets (MnO_2 NSs) as an oxidase mimic and catalytic label for AFB1 determination. As shown in Fig. 6A, the test (T) line of the strip was decorated with anti-AFB_1 antibody-conjugated MnO_2 NSs for capturing AFB_1. Impressively, thanks to the properties of MnO_2 NSs in catalyzing the oxidation of TMB, the TMB solution was added onto the T-line. When the target was added to the immunosensing device, the oxidation could provide a visual color signal which was inversely proportional to the AFB_1 concentration in the sample. The reported nanozyme-strip bioassay revealed an LOD of 15 pg mL^{-1} for AFB_1, over 100-fold lower than the maximum limit set by the European Union. On the other hand, both the instability of the colloidal nature of nanozymes and their complicated interactions with bio-receptors can limit nanozyme exploitation in LFA. In this light, it is crucial to rationally design nanozyme-based signal labels with features that facilitate easy functionalization, good dispersibility, distinctly visible color, and enzymatic activity.[101] These features are pivotal for increasing the applicability of nanozymes in LFA applications. A good example of this concept was prepared in another transition metal, CuCo, which was coated by polydopamine (PDA) with excellent biocompatibility, good adhesion, and rich functional groups (chinone, imine, and amine), leading to good hydrophilicity and binding ability with biomolecules.[100] In this protocol, the carboxyl-functionalized aptamers were conjugated with the CuCo@PDA nanozyme *via* amide condensation reactions. The fabricated probe was used on the surface of the T line and the difference of color with/without the presence of the target was the principle of

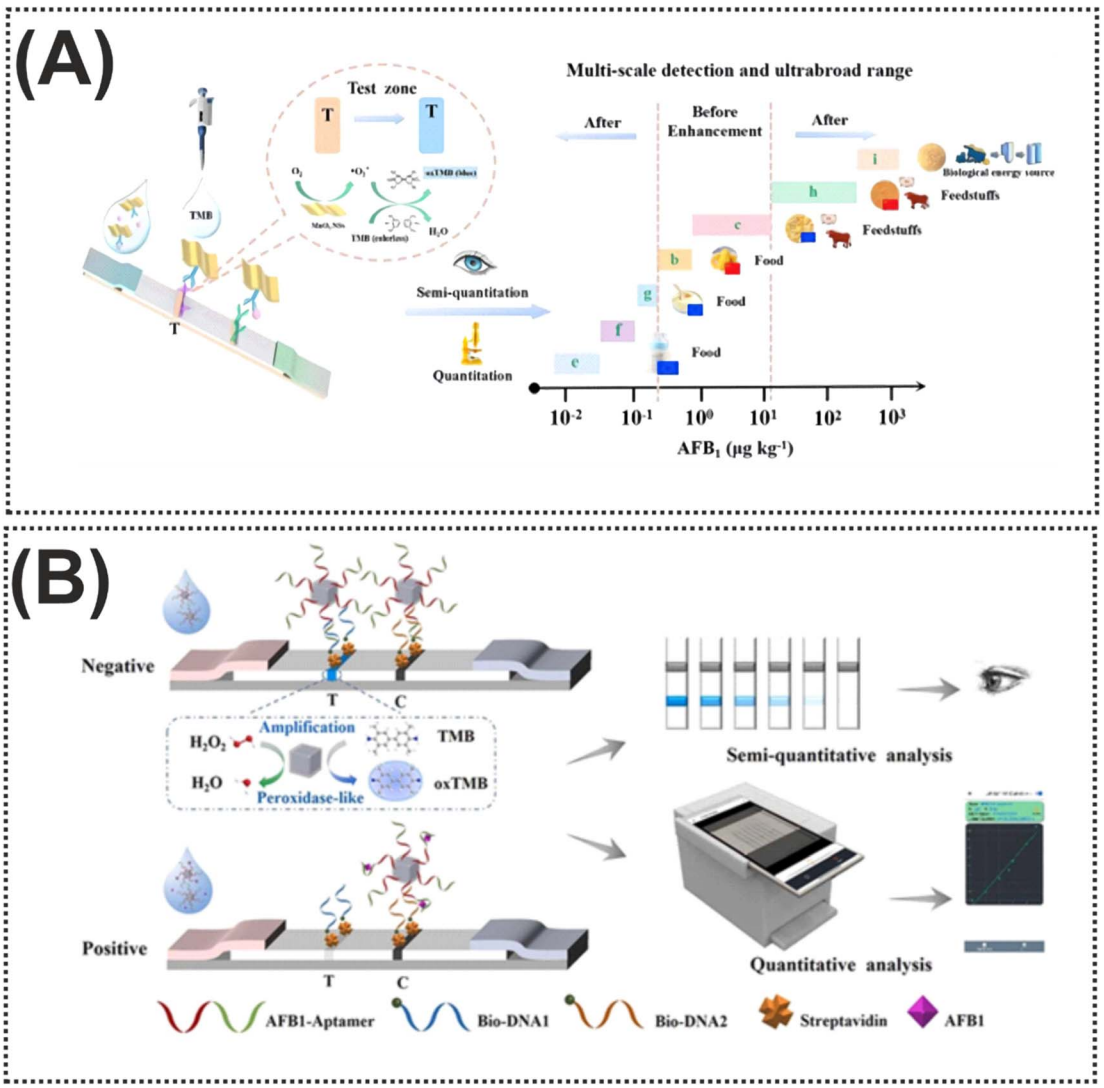

Fig. 6 (A) Schematic of the nanozyme-strip bioassay based on MnO_2 NSs for AFB_1 detection. Reproduced with permission from ref. 99. Copyright Elsevier Science, 2022. (B) Illustration of the use of CuCo@PDA in the structure of LFA for AFB_1 quantification. Reproduced with permission from ref. 100. Copyright Elsevier Science, 2024.

detection (Fig. 6B). Furthermore, the ability of the nanozyme to catalyze the oxidation of TMB-H_2O_2 could amplify the color change on the T-line. To illustrate this concept, the visual LOD was reduced to 0.1 ng mL^{-1} by TMB-H_2O_2 catalytic amplification. In 2024, Fan and colleagues[102] designed another functionalized nanozyme, flower-like L-cysteine-functionalized FeNi bimetallic nanoparticles (L-Cys-FeNiNPs), with excellent peroxidase-like catalytic activity in a colorimetric aptasensor for the detection of AFB_1. In the reported nanozyme, the peroxidase-like activity was attributed to the generation of superoxide radicals ($^{\bullet}O_2^-$) and holes (h^+) that were produced through the catalysis, and alongside that, the high selectivity of the probe was described by the conjugation of the specific aptamer with L-Cys-FeNiNPs *via* EDC/NHS chemistry and streptavidin–biotin interaction. Indeed, like the previous modification, the decoration of FeNiNPs with L-Cys can not only help increase the dispersibility and stability of the FeNiNPs, but also the biocompatibility and functionalization capability of nanozyme significantly improved. In the presence of the target, the reduction of the active sites of the L-Cys-FeNiNPs suppressed the TMB oxidation and reduced the color signal.

Along with metal-based nanozymes, the application of metal–organic framework (MOF) based nanozymes can be considered to have high potential for the quantification of AFB_1. Among different MOFs, porphyrin (PCN)-based organic linkers were employed for self-assembly with metal nodes, leading to the development of MOFs with different structures and functions. On the other hand, accessing the active sites within MOFs remains challenging. One of the efficient solutions is based on hybrid nanomaterials, which involves the use of platinum nanoparticles, Pt NPs, on two-dimensional support substrates.[103,104] As an example, Zhang *et al.*[105] reported a novel colorimetric approach exploiting the Pt@PCN-222 nanozyme, with oxygen vacancies, for AFB_1 detection. The detection principle of this study was based on the oxidation of the 2,2′-azinobis(3-ethylbenzthiazoline-6-sulfonic acid) (ABTS) substrate to produce a blue-green colored product. In the presence of the target, the binding of Pt@PCN-222 with the target caused inhibition which decreased the number of active Pt@PCN-222 conjugates available for the ABTS oxidation reaction. Another technique for addressing accessibility to the active sites of MOFs is based on the synthesis of NanoMOFs, which can accelerate substrate diffusion in catalytic MOF materials and this, in turn, provides greater external surface area and lower diffusion barriers. For instance, Peng and co-workers[106] developed a sensitive, reproducible, and accurate colorimetric immunoassay based on NanoPCN-223(Fe) with high peroxidase-like activity and excellent dispersion for AFB1 determination (Fig. 7). In the structure of the colorimetric technique, NanoPCN-223(Fe) produce color by catalyzing the oxidation of the colorless substrate TMB in the presence of H_2O_2. To illustrate this, through the catalysis process, the nanozyme generated hydroxyl radicals ($^{\bullet}OH$) from H_2O_2, which oxidize the TMB substrate, converting the colorless TMB to the blue ox-TMB. Under normal conditions, the conjugation of the nanozyme and the target inhibited the catalyzed oxidation of TMB which reduced the intensity of the color.

All things considered, the application of nanozymes based on metal nanoparticles and MOFs can be considered promising for aflatoxin detection. The investigation of these materials is based on two metal varieties, bimetallic and affordable materials, and alongside that, the amplification techniques can broaden our horizon on the performance of nanozymes in colorimetric approaches for the detection of aflatoxins.

4.1.2. Ochratoxin A. According to the International Agency for Research on Cancer, ochratoxin A, as possibly carcinogenic to humans (Group 2B), is classified as one of the significant mycotoxins. To elaborate, high chemical stability against heat treatments and hydrolysis through food processing makes it one of the most dangerous poisons for humans. This mycotoxin originates from the species of fungi including *Penicillium verrucosum*, *Aspergillus carbonarius*, *Aspergillus ochraceus*, and *Aspergillus niger*.[107,108] Over the last few decades, the advent of nanozymes has revolutionized multiple domains in the detection of OTA. Interestingly, the investigation of common structures of reported nanozymes can open new doors in terms of

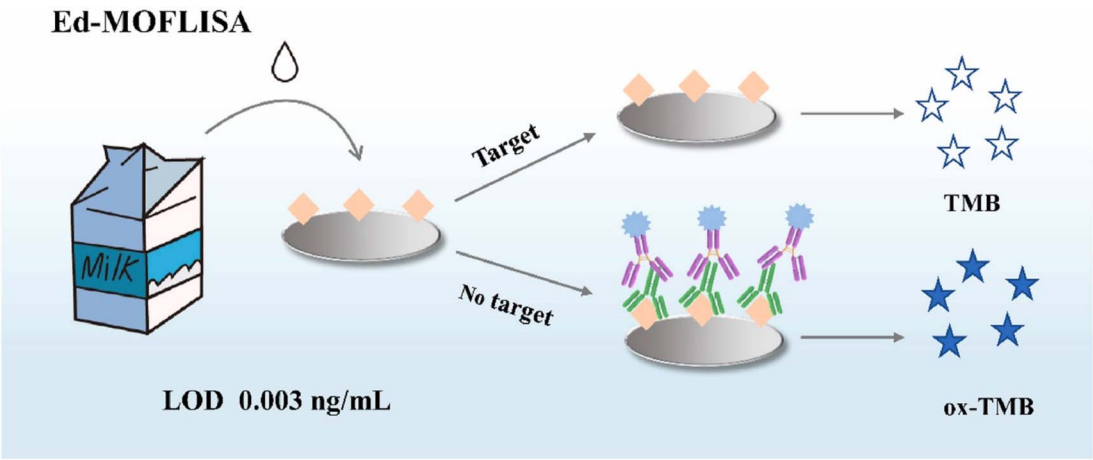

Fig. 7 Illustration of the application of NanoMOFs for colorimetric detection of AFB_1. Reproduced with permission from ref. 106. Copyright Elsevier Science, 2022.

quantification of OTA. One of the common structures is spinels which form huge families, and they consist of one or more metal elements. Among them, spinel-type metal oxides, with the formula of AB_2O_4, enjoy superior promoting nanozyme performance over other metal oxides due to their controllable structure, composition, valence, and morphology.[109,110] For example, Huang and co-workers[111] employed OTA-specific aptamers on the surface of manganese cation substituted cobalt oxide ($MnCo_2O_4$) for OTA determination. As shown in Fig. 8, the attachment of the aptamer on the surface of the nanozyme inhibited the nanozyme activity of spinel $MnCo_2O_4$ through the formation of an aptamer–target complex, presenting a new colorimetric aptasensor. Under normal conditions, the developed aptassay could detect OTA with an LOD of 0.08 ng mL^{-1}.

The distribution of cations among the octahedral and tetrahedral sites in the crystal structure can result in an inverse spinel structure, with a formula of $(AB)_4$, which demonstrates different electronic and magnetic features compared to the spinel structure.[112] Most recently, Liu and colleagues[113] improved the performance of an anti-spinel structure by using Au and Pt in the structure of Fe_3O_4, through an ionic liquid (IL) as the cross-linker, for capturing the synergistic interaction between the alloy atoms. In this work, the surface of the designed nanozyme was modified with complementary DNA for conjugating with a stainless steel mesh-aptamer. In the presence of the OTA, the binding of the target with the aptamer caused separation of the signaling probe ($AuPt@IL@Fe_3O_4$) and this, in turn, was added to a tube containing H_2O_2 and TMB for observing the color change. All in all, the inverse spinel and spinel structures introduce effective bioreceptor immobilization and high catalytic activity, increasing the performance of biosensors. However, the limited surface area and non-optimal electronic properties of spinel structures can restrict their application. In terms of inverse spinels, although magnetic features and high catalytic activity improve their performance, complex synthesis processes can limit their nanozyme-based application.

Along with these structures, tetragonal crystals and nanocube structures are other structures used in the development of nanozymes for OTA detection. To illustrate this, tetragonal crystal systems have been widely exploited in biosensors based on nanozymes owing to several advantages such as high surface area to volume ratio, stability, electronic features, high catalytic activity, and versatile functionalization.[114] Currently, one of the excellent examples of using nanozyme-based tetragonal crystal systems for detection of OTA was developed by Tian and co-workers.[115] In this protocol, the principle of this study was measuring the oxidase-mimicking activity of MnO_2 nanosheets. For this purpose, the decoration specific aptamer on the surface was exploited for capturing OTA, leading to the production of alkaline phosphatase-modified complementary DNA and the cascade reaction is triggered by the product (ascorbic acid) of alkaline phosphatase catalysis. The ascorbic acid reduced the oxidase-mimicking activity of MnO_2 nanosheets, leading to a pale color of the enzyme catalytic substrate. Another structure is a layered structure, with unique benefits, which can provide

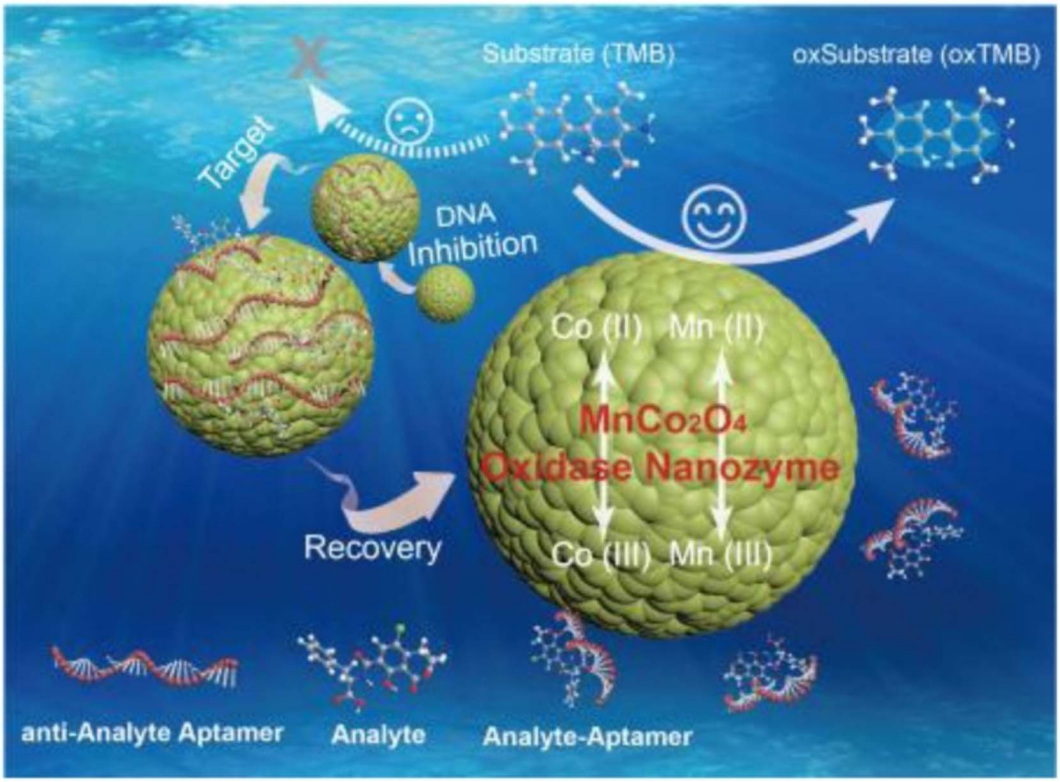

Fig. 8 Schematic of using $MnCo_2O_4$ in the structure of the colorimetric aptasensor for OTA determination. Reproduced with permission from ref. 111. Copyright Elsevier Science, 2018.

efficient nanozymes in the quantification of OTA. In 2020, Zhu *et al.*[116] fabricated a novel colorimetric immunosensor based on cobalt hydroxide nanoparticle $Co(OH)_2$ nanocages, with specific properties such as high surface area and high catalytic activity, for OTA quantification (Fig. 9). In detail, the microwell plate decorated with dopamine was modified with OTA and ab_1 and, followed, $Co(OH)_2$-ab_2 bounded to the prepared substrate. Under optimal circumstances, the difference of the color changes of TMB from the $Co(OH)_2$ nanocage in the absence of H_2O_2 could present an efficient biosensing platform with a linear range and detection limit of 0.5 ng L^{-1} to 5 μg L^{-1} and 0.26 ng L^{-1}, respectively. Despite the high surface area and catalytic activity of the nanocube structure, the stability issue under some conditions and aggregation of cubes can be considered important disadvantages of this structure. In addition, tetragonal crystal systems suffer from limited surface area.

4.2. Marine toxin detection

Marine toxins, as poisonous substances, can be considered as natural metabolites which are produced by numerous organisms such as bacteria, algae, and many marine invertebrates. Among them, algal toxins (including ciguatera toxin, domoic acid, and saxitoxin), invertebrate toxins, and some bacterial toxins may get concentrated in various organisms through the food web. The negative consequences of these toxins in both humans and animals are undeniable.[117,118] Importantly, various bioreceptors/receptors can improve the performance of nanozyme-based colorimetric biosensors for the determination of marine toxins. Antibodies, as one of the important bioreceptors, have been used in antibody–antigen interaction for presenting sensitivity and specificity detection approaches of marine toxins. Interestingly, the integration of nanozymes in the structures of colorimetric immunosensors can improve the analytical signal owing to the catalysis of the enzymatic reaction by nanozyme, which increases the color intensity. For example, Hendrickson and co-workers,[119] prepared a conjugated Au@Pt nanozyme with an antibody for enhancing the okadaic acid quantitative labeling. The tendency of Au@Pt nanozyme to conjugate with anti-mouse antibodies, rather than anti-okadaic acid antibodies, could provide excellent conditions for an indirect competitive immunoassay format. This phenomenon led to unproductive immune binding without signal change, resulting in improving the sensitivity of the immunoassay. When the target was added to the system, the okadaic acid competed with the okadaic acid on the conjugate pad for

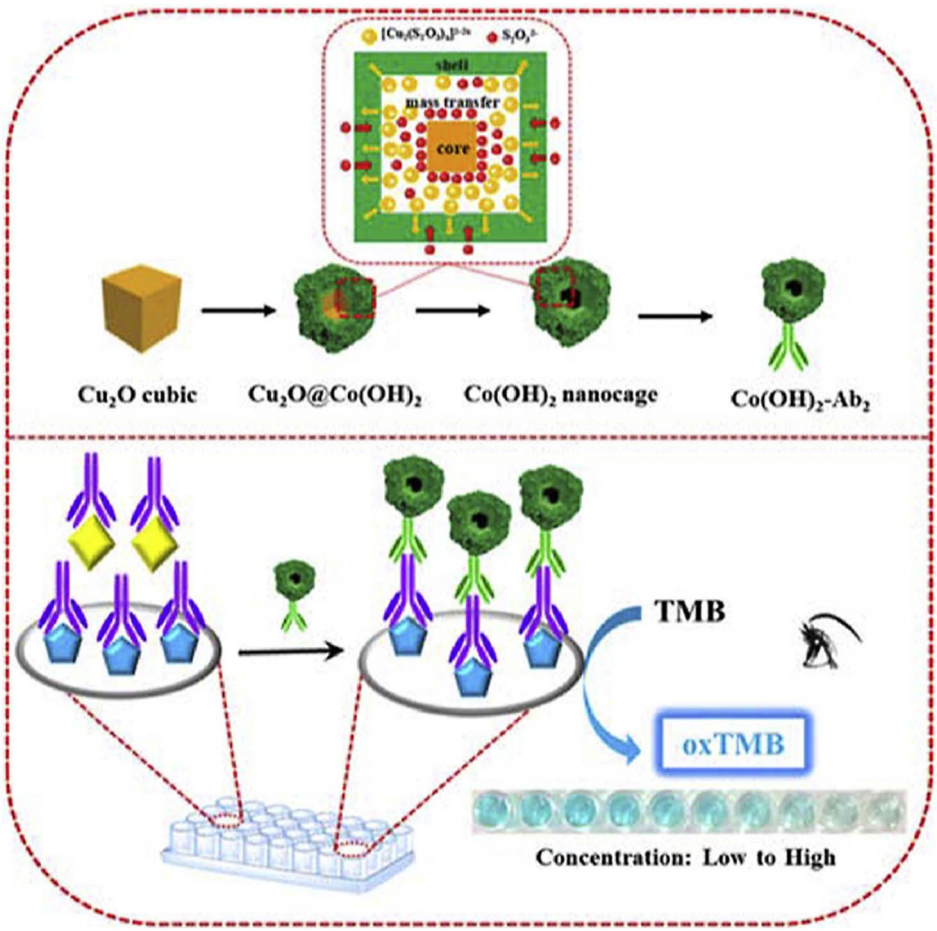

Fig. 9 Illustration of the colorimetric immunoassay based on Cu_2O nanocubes for the detection of OTA. Reproduced with permission from ref. 116. Copyright Elsevier Science, 2020.

binding with anti-okadaic acid antibodies and were immobilized on the T line of LFA.

The lack of chemical and thermal stability of antibodies, under harsh environmental conditions, can make them sensitive to degradation and denaturation. Furthermore, the high cost of production and purification of these bioreceptors can be considered another significant issue. In this regard, a competitive colorimetric biosensor was implanted in aptasensors based on AuNP nanozymes for sensitive and selective quantification of saxitoxin.[120] In this study, the competition of saxitoxin in samples with immobilized saxitoxin was the principle of the developed aptassay. To illustrate this, in the presence of the target, the separation of the specific aptamer from magnetic particles was conducted and this, in turn, led to triggering the hybridization chain reaction. The colorimetric signal was improved by amplifying the catalytic activity of the AuNP nanozymes. Similarly, in many colorimetric aptasensor studies, the adsorption of the aptamer could promote the enzyme-like activity of AuNPs for saxitoxin determination.[121,122] Elaborately, this phenomenon could enhance the surface negativity of nanozymes which increased the adsorption and diffusion of positively charged substrates such as TMB, improving the catalytic efficiency. In 2022, Li and colleagues[123] reported a novel aptasensor exploiting AuNPs@Fe^{2+} for multiple diarrhetic shellfish poison detection (Fig. 10). Indeed, the performance of the nanozyme, in terms of chemical stability and peroxidase-like activity, was improved by using Fe^{2+} in the structure of AuNPs. Furthermore, the high affinity of terminal-fixed aptamer (TF-DSP) was used in this study for the simultaneous detection of three diarrhetic shellfish poisons. Under normal circumstances, the catalysis of TMB/H_2O_2/acetic acid due to the excellent peroxidase-like activity and the brilliant selectivity of the aptamer could introduce a biosensing platform with a linear range and LOD of 0.4688–7.5 nM and 86.28 pM, respectively.

The complex immobilization process on the surface of nanozymes and the side effect of potential interferences, in real samples, can be considered the most important limitation of using aptamers in the nanozyme structure. In addition, in terms of overcoming the stability issues of combining antibodies with nanozymes, molecularly imprinted polymers (MIPs), as artificial antibody and antigen systems, have attracted considerable attention for marine toxin detection.[124,125] Most recently, Wu *et al.*[126] integrated an MIP with Au–Pt nanoparticles modified Fe_3O_4 magnetic nanozymes for introducing an efficient biosensor of saxitoxin. For this purpose, Au–Pt nanoparticles were loaded into Fe_3O_4 magnetic particles and, subsequently, thanks to the hydrolysis polymerization reaction, the decorated Fe_3O_4 magnetic nanozymes with MIPs were prepared. In the presence of the target, the catalyzed oxidation of TMB enabled the developed biosensing approach for detection of saxitoxin to achieve a detection limit of 3.1 nM. Potential interference in signal transduction, and durability and stability issues can be considered the most important limitations of MIPs. In order to address these limitations, scholars must pay special attention to the fabrication of optimized and compatible MIP-nanozyme platforms. For instance, Cho and colleagues[127] used peptides (as both the imprinting template and the signal peptide), instead of an antigen or aptamer, for competitive colorimetric quantification of saxitoxin. In this light, the exploitation of specific peptides of saxitoxin could overcome the difficulty of aptamer and antibody removal in biosensors based on the MIP-nanozyme. In addition, the integration of MIP with the specific peptide of saxitoxin was measured with AuNP/Co_3O_4@Mg/Al. In the presence of the target, the less specific peptide of saxitoxin was conjugated with MIP, leading to an intense color change.

4.3. Bacterial food toxins

Nowadays, bacterial food toxins, which are macromolecules mainly of protein origin, are one of the main issues in the realm of food safety. These microorganisms can produce toxins in food or once the pathogen has colonized the digestive tract. These types of toxins damage a specific organ of the host. To

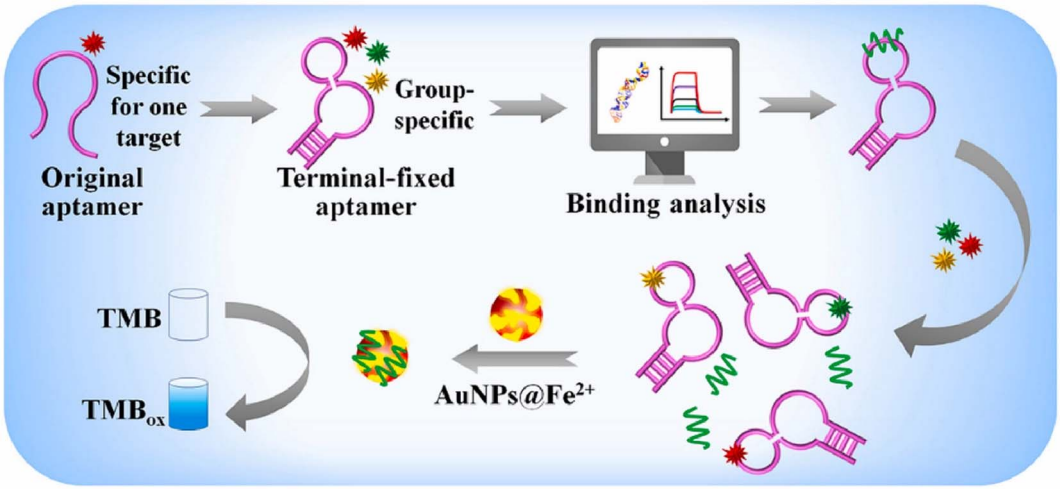

Fig. 10 Schematic of the colorimetric aptassay using AuNPs decorated with Fe^{2+} for multiple diarrhetic shellfish poison detection. Reproduced with permission from ref. 123. Copyright Elsevier Science, 2022.

illustrate this, such toxins cause foodborne diseases including vomiting, nausea, abdominal cramps, and diarrhea.[128,129] Despite the fact that the field of research on the detection of bacterial toxins is very wide, researchers attempted the use of different nanomaterials in the structures of nanozymes for amplification of detection signals. Various forms of Au-based nanomaterials such as AuNPs and gold nanostars (AuNSs) have been exploited as one of the important nanomaterials to amplify the signal due to several benefits such as excellent stability, repeatability, and accuracy. These nanomaterials gained great attention due to their ability to couple and integrate with different bioreceptors and nanomaterials for acting as nanozymes through chemical bonds and electrostatic adsorption. As for labelling nanomaterials, Ren *et al.*[130] used the seed growth method for assembling AuNSs in the structure of Mn/Fe-MIL(53) for introducing an efficient nanozyme in the colorimetric and SERS detection of Shiga toxin type II. As shown in Fig. 11A, in terms of construction of signal probes which could oxidize colorless TMB into the blue color oxTMB, the surface of Mn/Fe-MIL(53) was decorated with AuNSs for providing an excellent substrate for immobilization of SH-complementary DNA, through Au–S bonding. In addition, to obtain the capturing probe, streptavidin-labeled magnetic beads were modified with a specific biotin-labeled aptamer. In the presence of the target, the conjugation of the aptamer with the target facilitates release of signal probes from the complex

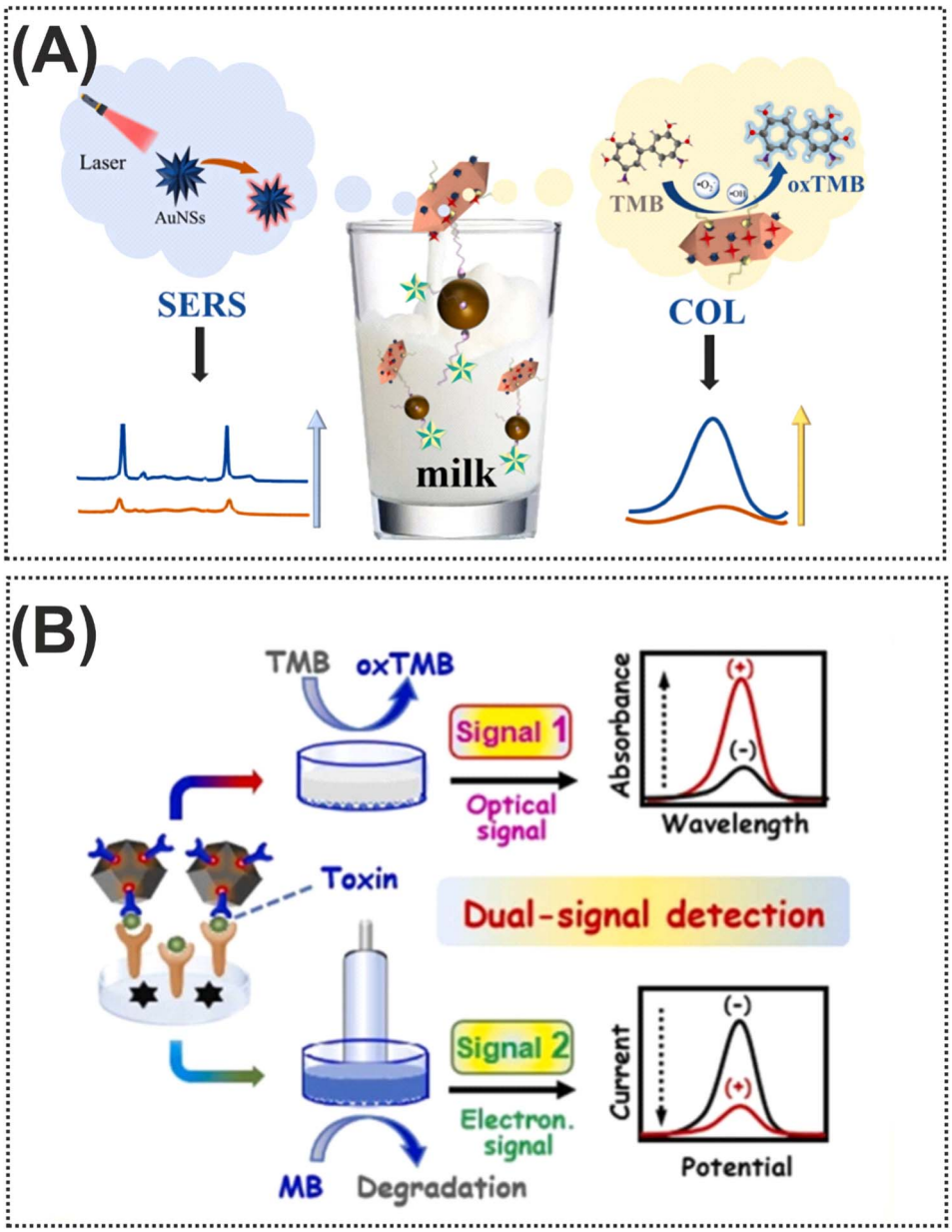

Fig. 11 (A) Representation of the dual-mode colorimetric and SERS biosensor based on Mn/Fe-MIL(53)@AuNSs for Shiga toxin type II detection. Reproduced with permission from ref. 130. (B) Illustration of dual-signal electrochemical and colorimetric detection of *Staphylococcus aureus* enterotoxin B.[131] Copyright Elsevier Science, 2024.

Table 1 Comparison report of colorimetric sensors with nanozymes for the detection of different biotoxins

Nanozymes	Enzyme activity	Substrate	Target	Linear range	LOD	Ref.
Au@HgNPs	OXD	TMB	AFB_1	0.125 to 87.5 μg L^{-1}	0.08 μg L^{-1}	91
CHNPs	OXD	TMB	AFB_1	1 pg mL^{-1} to 20 ng mL^{-1}	0.73 pg mL^{-1}	92
Au–Pt	OXD	TMB	AFB_1	0.1 to 500 ng mL^{-1}	5 pg mL^{-1}	93
MoS_2/Au	POD	TMB	AFB_1	1 to 100 ng mL^{-1}	0.25 ng mL^{-1}	141
Pt–CN	POD	TMB	AFB_1	1.0 pg mL^{-1} to 10 ng mL^{-1}	0.22 pg mL^{-1}	95
Ag@Au IP6	POD	TMB	AFB_1	2 pg L^{-1} to 200 pg L^{-1}	0.58 pg L^{-1}	98
MnO_2 NSs	OXD	TMB	AFB_1	0.01 to 150 ng mL^{-1}	0.015 ng mL^{-1}	99
CuCo@PDA	POD	TMB	AFB_1	0.01 to 50 ng mL^{-1}	2.2 pg mL^{-1}	100
FeNiNPs	POD	TMB	AFB_1	0.12 to 2 μg mL^{-1}	36.57 ng mL^{-1}	102
Pt@PCN-222	OXD	ABTS	AFB_1	0.1 to 10 ng mL^{-1}	0.074 μg L^{-1}	142
NanoPCN-223	POD	TMB	AFB_1	0.05 to 10 ng mL^{-1}	0.003 ng mL^{-1}	106
$MnCo_2O_4$	OXD	TMB	OTA	0.1 to 10 ng mL^{-1}	0.08 ng mL^{-1}	111
Fe_3O_4	POD	TMB	OTA	5 to 100 ng mL^{-1}	0.078 ng mL^{-1}	113
MnO_2 NSs	OXD	TMB	OTA	1.25 to 250 nM	0.069 nM	115
Cu_2O nanocubes	OXD	TMB	OTA	0.5 ng L^{-1} to 5 mg L^{-1}	0.26 ng L^{-1}	116
Au@Pt	POD	TMB	Okadaic acid	0.8 to 6.8 ng L^{-1}	0.5 ng L^{-1}	119
AuNPs	POD	TMB	Saxitoxin	78.13 to 2500 pM	42.46 pM	120
AuNPs@Fe^{2+}	POD	TMB	Okadaic acid, dinophysistoxin-1, and dinophysistoxin-2	4688 to 7.5 nM	86.28 pM	123
Fe_3O_4@Au–Pt	OXD	TMB	Saxitoxin	0.01 to 100 μM	3.1 nM	126
AuNP/Co_3O_4@Mg/Al cLDH	POD	TMB	Saxitoxin	0 to1000 ng mL^{-1}	3.17 ng mL^{-1}	127
Mn/Fe-MIL(53)@AuNSs	POD	TMB	Shiga toxin type II	0.05 to 500 ng mL^{-1}	26 pg mL^{-1}	130
AuPt@Fe–N–C	POD	TMB	*Staphylococcus aureus* enterotoxin B	0.0002 to 10.000 ng mL^{-1}	0667 pg mL^{-1}	131
Rh	POD	TMB	Staphylococcal enterotoxin B	0 to 2 ng mL^{-1}	1.2 pg mL^{-1}	132

resulting in an enhancement of SERS and colorimetric signals. In the reported dual-mode, the integration of SERS and colorimetric approaches introduced complementary and validated results, improving the reliability of the Shiga toxin type II detection. In another example of Au-based nanozymes, Liang and co-workers[131] designed a novel dual-signal probe (AuPt nanoparticle-loaded single atom nanocomposite, AuPt@Fe–N–C) for *Staphylococcus aureus* enterotoxin B quantification (Fig. 11B). For this purpose, ab_1 was immobilized on the surface of AuPt@Fe–N–C and this was used for the sandwich structure. In addition to the target, AB_1-*Staphylococcus aureus* enterotoxin B-ab_2, which oxidises TMB from colorless to blue, had a detection limit of 0.066 7 pg mL^{-1} in 96-well plates. Along with Au-based nanozymes, the unique properties and structure of rhodium (Rh), a non-toxic transition metal, were exploited for staphylococcal enterotoxin B determination in milk samples.[132] The implementation of Rh, with peroxidase-like catalytic activity, in the sensing zone of LFA could enable detection of staphylococcal enterotoxin B with a detection limit as low as 1.2 pg mL^{-1}.

5. Theranostic applications of nanozymes for biotoxins

Nanozymes' catalytic theranostics introduces an innovative and novel strategy for theranostic platforms, integrating detection and treatment in a single system.[133] The importance of these platforms is highlighted in preventing the spread of biotoxins in contamination outbreaks by intervention to neutralize biotoxins and monitoring them.[134] For the detection of biotoxins, catalytic color changing reactions are conducted for achieving sensitive colorimetric sensors, Table 1. In terms of neutralization and degradation of biotoxins, the oxidation and hydrolysis of biotoxins to break these toxic by-products down into non-toxic components by using nanozymes is an efficient strategy for rendering them harmless.[135,136] Numerous techniques are exploited for biotoxin degradation such as the UV method for marine biotoxins demonstrating resistance to photodegradation. On the other hand, high performance degradation with UV/$S_2O_8^{2-}$ and UV/H_2O_2 was achieved.[137,138] In addition, biodegrading ATX-a into a nontoxic byproduct by *Bacillus* strains such as *Bacillus flexus* SSZ01 and *Bacillus* strain AMRI-03 can lead to a high performance method for water treatment like rapid degradation of saxitoxins, which is directly and indirectly associated with food safety.[139] Furthermore, MOF-derived nanozymes were used as high potential materials in the neutralization process.[140] Future research should be focused on the theranostic application of nanozymes for biotoxins due to a lack of research studies in this field. In other words, this field can advance biosensors and detoxification systems, managing biotoxin threats in different environments and food matrices.

6. Conclusions and future perspectives

Numerous attempts have been undertaken to control biotoxins, however, their contamination remains largely inevitable.

Therefore, there is an urgent need for research to explore biosensors for the rapid, sensitive, and convenient detection of biotoxins, given the detrimental impact of biotoxins on human health and food safety. So, as described in this literature update, owing to their favorable catalytic activity, excellent stability, and low cost, nanozymes and nanozyme-based biosensors have been extensively exploited to identify different biotoxins in food and environmental samples. In particular, the combination of colorimetric biosensors and nanozymes to construct an innovative biosensing scaffold provides a promising outlook in convenient, sensitive, and rapid quantification of various biotoxins. Herein, we have discussed the production, characteristics, and application of nanozymes in colorimetric biosensors, focusing on their diverse catalytic activities. Furthermore, a comprehensive overview of the research conducted on the utilization of nanozyme-based colorimetric biosensors for the identification of biotoxins is provided. Through deliberating the sensing approaches employed using nanozyme-based colorimetric biosensors, it becomes evident that these biosensors play crucial roles in the rapid diagnosis of biotoxins. Besides, we highlight the recent advancements in portable technologies, including hydrogels and paper-based platforms, which can be integrated with smartphones to enable on-site detection. Although nanozyme-based colorimetric biosensors possess the features of fast response, simple operation, high sensitivity, and low cost, they still have some challenges in several aspects.

(i) Due to the inferior catalytic efficiency of nanozymes in comparison with natural enzymes, the application of nanozymes with multiple catalytic and high activity can be considered as one of the efficient strategies. Indeed, multiple catalytic activities including peroxidase-like, oxidase-like, and catalase-like activities can improve the performance of nanozymes. Furthermore, the concept of highly activated nanozymes is achieved by the integration of nanozymes with different nanomaterials. Also, the lower selectivity of nanozymes towards targets restricts specific recognition in the detection process. Consequently, the development of novel nanozymes with enhanced specificity could involve the integration of biomimetic recognition elements, such as MIPs, and exploring additional technical approaches holds promise for future advancements in this area.

(ii) Currently, an increasing number of studies are focusing on nanozymes exhibiting multiple enzyme activities. However, the utilization of nanozymes with multiple enzyme performances in colorimetric biosensors predominantly depends on their POD and OXD-like activities. Regulating the predominant activity of nanozymes with multiple enzyme-like functions simultaneously poses a significant challenge. This task necessitates a more precise comprehension of the catalytic mechanisms underlying various enzyme activities, along with a thorough understanding of the primary factors influencing these activities.

(iii) The catalytic reactions occur in specific regions on the nanozyme's surface which are considered as active places. Generally, these active places are operated in a similar manner to the active sites in natural enzymes. However, their function and structure can differ owing to the basic differences between biological macromolecules and nanomaterials.[143] Elaborately, the presence of a small number of amino acids can allow natural enzymes to directly interact with the substrate. Hydrophobic interactions and hydrogen bonding are the most important of these interactions, resulting in high efficiency and specificity of the substrate. On the other hand, specific atoms or clusters of atoms on the surface of nanozymes act as active places. In detail, specific functional groups or metal ions can mimic the catalytic functions of natural enzymes. In addition, the chemical composition, size, and shape of nanozymes can impact their catalytic activity.[144]

To sum up, the investigation of nanozymes and nanozyme-based colorimetric biosensors represents merely the initial phase of a vast field of study. Nevertheless, it is evident that these biosensors exhibit significant promise in applications and merit further investigation. As research progresses and nanozyme-based colorimetric biosensors continue to evolve, it is anticipated that more cutting-edge technologies and portable devices will be developed and extensively employed to safeguard food and environmental integrity.

Data availability

No data were used for the research described in the article.

Conflicts of interest

There are no conflicts to declare.

Acknowledgements

This work was financially supported by Jiyang College of Zhejiang A&F University (RQ1911F12) and Scientific Research Project of Education Department of Zhejiang Province (Y202352649).

References

1 M. Mahmoudpour, J. Ezzati Nazhad Dolatabadi, M. Torbati, A. Pirpour Tazehkand, A. Homayouni-Rad and M. de la Guardia, *Biosens. Bioelectron.*, 2019, **143**, 111603.
2 M. Mahmoudpour, J. Ezzati Nazhad Dolatabadi, M. Torbati and A. Homayouni-Rad, *Biosens. Bioelectron.*, 2019, **127**, 72–84.
3 J. Nicolas, R. L. Hoogenboom, P. J. Hendriksen, M. Bodero, T. F. Bovee, I. M. Rietjens and A. Gerssen, *Global Food Secur.*, 2017, **15**, 11–21.
4 M.-L. Liu, X.-M. Liang, M.-Y. Jin, H.-W. Huang, L. Luo, H. Wang, X. Shen and Z.-L. Xu, *J. Agric. Food Chem.*, 2024, **72**, 10753–10771.
5 F. Javaheri-Ghezeldizaj, M. Mahmoudpour, R. Yekta and J. Ezzati Nazhad Dolatabadi, *J. Mol. Liq.*, 2020, **310**, 113259.
6 C. Lin, Z.-S. Liu, C.-Y. Tan, Y.-P. Guo, L. Li, H.-L. Ren, Y.-S. Li, P. Hu, S. Gong and Y. Zhou, *Environ. Sci. Pollut. Res.*, 2015, **22**, 1545–1553.
7 D. Liu, in *Molecular Medical Microbiology*, Elsevier, 2024, pp. 933–944.

8 P. Sadeghi, H. Sohrabi, M. R. Majidi, A. Eftekhari, F. Zargari, M. de la Guardia and A. A. Mokhtarzadeh, *Trac. Trends Anal. Chem.*, 2024, 117722.
9 Y. Liu and F. Wu, *Environ. Health Perspect.*, 2010, **118**, 818–824.
10 S. Siva, J.-O. Jin, I. Choi and M. Kim, *Biosens. Bioelectron.*, 2023, **219**, 114845.
11 M. Mahmoudpour, S. Ding, Z. Lyu, G. Ebrahimi, D. Du, J. Ezzati Nazhad Dolatabadi, M. Torbati and Y. Lin, *Nano Today*, 2021, **39**, 101177.
12 Z. Karimzadeh, M. Mahmoudpour, E. Rahimpour and A. Jouyban, *Adv. Colloid Interface Sci.*, 2022, **305**, 102705.
13 T. A. Rocha-Santos, *Trac. Trends Anal. Chem.*, 2014, **62**, 28–36.
14 Z. Golsanamlou, M. Mahmoudpour, J. Soleymani and A. Jouyban, *Crit. Rev. Anal. Chem.*, 2023, **53**, 1116–1131.
15 Z. Khoshbin, M. Moeenfard, K. Abnous and S. M. Taghdisi, *Food Chem.*, 2024, **433**, 137355.
16 L. Lu, R. Yu and L. Zhang, *Food Chem.*, 2023, **421**, 136205.
17 R. L. F. Melo, F. S. Neto, D. N. Dari, B. C. C. Fernandes, T. M. Freire, P. B. A. Fechine, J. M. Soares and J. C. S. Dos Santos, *Int. J. Biol. Macromol.*, 2024, 130817.
18 T. Vyas, V. Singh, P. Kodgire and A. Joshi, *Crit. Rev. Biotechnol.*, 2023, **43**, 521–539.
19 J. Qin, N. Guo, J. Yang and J. Wei, *Food Chem.*, 2024, 139019.
20 A. Baranwal, R. Shukla and V. Bansal, *Trac. Trends Anal. Chem.*, 2024, 117573.
21 L. Yang, X. Xu, Y. Song, J. Huang and H. Xu, *Chem. Eng. J.*, 2024, **487**, 150612.
22 Z. Chi, Q. Wang and J. Gu, *Analyst*, 2023, **148**, 487–506.
23 B. Unnikrishnan, C.-W. Lien, H.-W. Chu and C.-C. Huang, *J. Hazard. Mater.*, 2021, **401**, 123397.
24 Y. Huang, J. Ren and X. Qu, *Chem. Rev.*, 2019, **119**, 4357–4412.
25 H. Wei, L. Gao, K. Fan, J. Liu, J. He, X. Qu, S. Dong, E. Wang and X. Yan, *Nano Today*, 2021, **40**, 101269.
26 L. Zhang, H. Wang and X. Qu, *Adv. Mater.*, 2024, **36**, 2211147.
27 Z. Li, W. Liu, P. Ni, C. Zhang, B. Wang, G. Duan, C. Chen, Y. Jiang and Y. Lu, *Chem. Eng. J.*, 2022, **428**, 131396.
28 Z. Lou, S. Zhao, Q. Wang and H. Wei, *Anal. Chem.*, 2019, **91**, 15267–15274.
29 K. Fan, J. Xi, L. Fan, P. Wang, C. Zhu, Y. Tang, X. Xu, M. Liang, B. Jiang, X. Yan and L. Gao, *Nat. Commun.*, 2018, **9**, 1440.
30 P. Zhang, D. Sun, A. Cho, S. Weon, S. Lee, J. Lee, J. W. Han, D.-P. Kim and W. Choi, *Nat. Commun.*, 2019, **10**, 940.
31 S. Pandit and M. De, *Nanoscale Adv.*, 2021, **3**, 5102–5110.
32 H. Sun, A. Zhao, N. Gao, K. Li, J. Ren and X. Qu, *Angew. Chem., Int. Ed.*, 2015, **54**, 7176–7180.
33 M. Mahmoudpour, J. E. N. Dolatabadi, M. Hasanzadeh, A. H. Rad, M. Torbati and F. Seidi, *RSC Adv.*, 2022, **12**, 29602–29612.
34 M. S. Kim, S. Cho, S. H. Joo, J. Lee, S. K. Kwak, M. I. Kim and J. Lee, *ACS Nano*, 2019, **13**, 4312–4321.
35 Z. Wang, Z. Xu, X. Xu, J. Xi, J. Han, L. Fan and R. Guo, *Colloids Surf., B*, 2022, **217**, 112671.
36 F. Li, J. Jiang, H. Peng, C. Li, B. Li and J. He, *Sens. Actuators, B*, 2022, **369**, 132334.
37 L. Zhu, W. Zeng, Y. Li, Y. Han, J. Wei and L. Wu, *Sci. Total Environ.*, 2024, **921**, 171236.
38 X. Liang, X. Wang, Y. Zhang, B. Huang and L. Han, *J. Agric. Food Chem.*, 2022, **70**, 3898–3906.
39 X. Zhang, Y. Xu, X. Wang, T. Chen, Q. Yao, S. Chang, X. Guo, X. Liu, H. Wu and Y. Cui, *Food Chem.*, 2024, 140710.
40 C. Lu, L. Tang, F. Gao, Y. Li, J. Liu and J. Zheng, *Biosens. Bioelectron.*, 2021, **187**, 113327.
41 S. Naveen Prasad, P. Weerathunge, M. N. Karim, S. Anderson, S. Hashmi, P. D. Mariathomas, V. Bansal and R. Ramanathan, *Anal. Bioanal. Chem.*, 2021, **413**, 1279–1291.
42 D. Li, D. Dai, G. Xiong, S. Lan and C. Zhang, *Small*, 2023, **19**, 2205870.
43 P. T. Nguyen, J. Lee, A. Cho, M. S. Kim, D. Choi, J. W. Han, M. I. Kim and J. Lee, *Adv. Funct. Mater.*, 2022, **32**, 2112428.
44 Y. Lin, C. Xu, J. Ren and X. Qu, *Angew. Chem.*, 2012, **51**, 12579–12583.
45 L. Gao, J. Zhuang, L. Nie, J. Zhang, Y. Zhang, N. Gu, T. Wang, J. Feng, D. Yang, S. Perrett and X. Yan, *Nat. Nanotechnol.*, 2007, **2**, 577–583.
46 R. André, F. Natálio, M. Humanes, J. Leppin, K. Heinze, R. Wever, H. C. Schröder, W. E. Müller and W. Tremel, *Adv. Funct. Mater.*, 2011, **21**, 501–509.
47 A. B. Ganganboina and R.-a. Doong, *Sens. Actuators, B*, 2018, **273**, 1179–1186.
48 H. Li, S. Zhao, Z. Wang and F. Li, *Small*, 2023, **19**, 2206465.
49 L. Han, H. Zhang, D. Chen and F. Li, *Adv. Funct. Mater.*, 2018, **28**, 1800018.
50 Q. Liu, A. Zhang, R. Wang, Q. Zhang and D. Cui, *Nano-Micro Lett.*, 2021, **13**, 1–53.
51 Z. Karimzadeh, M. Mahmoudpour, M. d. l. Guardia, J. Ezzati Nazhad Dolatabadi and A. Jouyban, *Trac. Trends Anal. Chem.*, 2022, **152**, 116622.
52 Z. Karimzadeh, M. Mahmoudpour, E. Rahimpour and A. Jouyban, *RSC Adv.*, 2024, **14**, 9571–9586.
53 Z. Karimzadeh, A. Jouyban, A. Ostadi, A. Gharakhani and E. Rahimpour, *Anal. Chim. Acta*, 2022, **1227**, 340252.
54 X. Zhang, G. Li, D. Wu, X. Li, N. Hu, J. Chen, G. Chen and Y. Wu, *Biosens. Bioelectron.*, 2019, **137**, 178–198.
55 X. Huang, S. Zhang, Y. Tang, X. Zhang, Y. Bai and H. Pang, *Coord. Chem. Rev.*, 2021, **449**, 214216.
56 W. He, Z. Li, S. Lv, M. Niu, W. Zhou, J. Li, R. Lu, H. Gao, C. Pan and S. Zhang, *Chem. Eng. J.*, 2021, **409**, 128274.
57 K. Zhang, K. Dai, R. Bai, Y. Ma, Y. Deng, D. Li, X. Zhang, R. Hu and Y. Yang, *Chin. Chem. Lett.*, 2019, **30**, 664–667.
58 Z. Sun, M. Wang, J. Fan, R. Feng, Y. Zhou and L. Zhang, *Adv. Compos. Hybrid Mater.*, 2021, **4**, 1322–1329.
59 Y. Su, M. Lu, R. Su, W. Zhou, X. Xu and Q. Li, *Chin. Chem. Lett.*, 2022, **33**, 2573–2578.
60 L. Zheng, F. Wang, C. Jiang, S. Ye, J. Tong, P. Dramou and H. He, *Coord. Chem. Rev.*, 2022, **471**, 214760.
61 X. Niu, B. Liu, P. Hu, H. Zhu and M. Wang, *Biosensors*, 2022, **12**, 251.

62 H. Deng, Y. Zhang, X. Cai, Z. Yin, Y. Yang, Q. Dong, Y. Qiu and Z. Chen, *Small*, 2024, **20**, 2306155.
63 Z. Wang, M. Li, H. Bu, D. S. Zia, P. Dai and J. Liu, *Mater. Chem. Front.*, 2023, **7**, 3625–3640.
64 M.-L. Ye, Y. Zhu, Y. Lu, L. Gan, Y. Zhang and Y.-G. Zhao, *Talanta*, 2021, **230**, 122299.
65 Y. Song, K. Qu, C. Zhao, J. Ren and X. Qu, *Adv. Mater.*, 2010, **22**, 2206–2210.
66 Z. Lyu, J. Zhou, S. Ding, D. Du, J. Wang, Y. Liu and Y. Lin, *Trac. Trends Anal. Chem.*, 2023, 117280.
67 X. Zhang, C. Sun, R. Li, X. Jin, Y. Wu and F. Fu, *Anal. Chem.*, 2023, **95**, 5024–5033.
68 H. Li, M. Sun, H. Gu, J. Huang, G. Wang, R. Tan, R. Wu, X. Zhang, S. Liu and L. Zheng, *Small*, 2023, **19**, 2207036.
69 M. Comotti, C. Della Pina, R. Matarrese and M. Rossi, *Angew. Chem., Int. Ed.*, 2004, **43**, 5812–5815.
70 Y. Peng, M. Huang, L. Chen, C. Gong, N. Li, Y. Huang and C. Cheng, *Nano Res.*, 2022, **15**, 8783–8790.
71 M. Ren, Y. Zhang, L. Yu, L. Qu, Z. Li and L. Zhang, *Talanta*, 2023, **255**, 124219.
72 X. Zhou, M. Wang, J. Chen and X. Su, *Talanta*, 2022, **245**, 123451.
73 S. Khajir, Z. Karimzadeh, M. Khoubnasabjafari, V. Jouyban-Gharamaleki, E. Rahimpour and A. Jouyban, *J. Pharm. Biomed. Anal.*, 2023, **223**, 115141.
74 S. Singh, *Front. Chem.*, 2019, **7**, 46.
75 S. Singh, *Int. J. Biol. Macromol.*, 2024, 129374.
76 D. Mehta, P. Sharma and S. Singh, *Colloids Surf., B*, 2023, **231**, 113531.
77 M. S. Lord, J. F. Berret, S. Singh, A. Vinu and A. S. Karakoti, *Small*, 2021, **17**, 2102342.
78 A. K. Singh, K. Bijalwan, N. Kaushal, A. Kumari, A. Saha and A. Indra, *ACS Appl. Nano Mater.*, 2023, **6**, 8036–8045.
79 M. Zhang, Y. Wang, N. Li, D. Zhu and F. Li, *Biosens. Bioelectron.*, 2023, **237**, 115554.
80 M. Jia, F. Xu, F. Zhai, X. Yu and M. Du, *J. Colloid Interface Sci.*, 2024, **653**, 1805–1816.
81 C. P. Liu, T. H. Wu, C. Y. Liu, K. C. Chen, Y. X. Chen, G. S. Chen and S. Y. Lin, *Small*, 2017, **13**, 1700278.
82 S. Guo, Y. Han and L. Guo, *Catal. Surv. Asia*, 2020, **24**, 70–85.
83 Z. Wang, X. Shen, X. Gao and Y. Zhao, *Nanoscale*, 2019, **11**, 13289–13299.
84 R. Zhang, B. Xue, Y. Tao, H. Zhao, Z. Zhang, X. Wang, X. Zhou, B. Jiang, Z. Yang and X. Yan, *Adv. Mater.*, 2022, **34**, 2205324.
85 W. Yang, X. Yang, L. Zhu, H. Chu, X. Li and W. Xu, *Coord. Chem. Rev.*, 2021, **448**, 214170.
86 A. Casu, M. Camardo Leggieri, P. Toscano and P. Battilani, *Compr. Rev. Food Sci. Food Saf.*, 2024, **23**, e13323.
87 M.-H. Moosavy, M. Hasanzadeh, J. Soleymani and A. Mokhtarzadeh, *Anal. Methods*, 2019, **11**, 3910–3919.
88 Y. Zhang, X. Chen, X. Xie, D. Li, Y. Fan, B. Huang and X. Yang, *Curr. Anal. Chem.*, 2024, **20**, 242–254.
89 Z. Xue, Y. Zhang, W. Yu, J. Zhang, J. Wang, F. Wan, Y. Kim, Y. Liu and X. Kou, *Anal. Chim. Acta*, 2019, **1069**, 1–27.
90 C. Peng, R. Pang, J. Li and E. Wang, *Adv. Mater.*, 2024, **36**, 2211724.
91 X. Zhao, Q. Li, H. Li, Y. Wang, F. Xiao, D. Yang, Q. Xia and Y. Yang, *Food Chem.*, 2023, **424**, 136443.
92 W. Lai, J. Guo, Y. Wang, Y. Lin, S. Ye, J. Zhuang and D. Tang, *Talanta*, 2022, **247**, 123546.
93 L. Wu, M. Zhou, Y. Wang and J. Liu, *J. Hazard Mater.*, 2020, **399**, 123154.
94 W. Jiang, Q. Yang, H. Duo, W. Wu and X. Hou, *Food Chem.*, 2024, 138917.
95 S. Huang, W. Lai, B. Liu, M. Xu, J. Zhuang, D. Tang and Y. Lin, *Spectrochim. Acta, Part A*, 2023, **284**, 121782.
96 N. Ullah, T. A. Bruce-Tagoe, G. A. Asamoah and M. K. Danquah, *Int. J. Mol. Sci.*, 2024, **25**, 5959.
97 S. Ganguly and S. Margel, *Talanta*, 2023, 100243.
98 X. Tan, K. Kang, R. Zhang, J. Dong, W. Wang and W. Kang, *Sens. Actuators, B*, 2024, **412**, 135854.
99 X. Cai, M. Liang, F. Ma, Z. Zhang, X. Tang, J. Jiang, C. Guo, S. R. Mohamed, A. A. Goda and D. H. Dawood, *Food Chem.*, 2022, **377**, 131965.
100 X. Zhu, J. Tang, X. Ouyang, Y. Liao, H. Feng, J. Yu, L. Chen, Y. Lu, Y. Yi and L. Tang, *J. Hazard. Mater.*, 2024, **465**, 133178.
101 T. Bu, P. Jia, X. Sun, Y. Liu, Q. Wang and L. Wang, *Sens. Actuators, B*, 2020, **320**, 128440.
102 Y. Fan, D. Li, X. Xie, Y. Zhang, L. Jiang, B. Huang and X. Yang, *Microchem. J.*, 2024, **197**, 109842.
103 X. Zhang, M. C. Wasson, M. Shayan, E. K. Berdichevsky, J. Ricardo-Noordberg, Z. Singh, E. K. Papazyan, A. J. Castro, P. Marino and Z. Ajoyan, *Coord. Chem. Rev.*, 2021, **429**, 213615.
104 P. Li, R. C. Klet, S.-Y. Moon, T. C. Wang, P. Deria, A. W. Peters, B. M. Klahr, H.-J. Park, S. S. Al-Juaid and J. T. Hupp, *Chem. Commun.*, 2015, **51**, 10925–10928.
105 S. Zhang, H. Li, Q. Xia, D. Yang and Y. Yang, *J. Food Sci.*, 2024, **89**, 3618–3628.
106 S. Peng, K. Li, Y.-x. Wang, L. Li, Y.-H. Cheng and Z. Xu, *Anal. Biochem.*, 2022, **655**, 114829.
107 C. Jiang, L. Lan, Y. Yao, F. Zhao and J. Ping, *Trac. Trends Anal. Chem.*, 2018, **102**, 236–249.
108 Y. Alhamoud, D. Yang, S. S. F. Kenston, G. Liu, L. Liu, H. Zhou, F. Ahmed and J. Zhao, *Biosens. Bioelectron.*, 2019, **141**, 111418.
109 Q. Zhao, Z. Yan, C. Chen and J. Chen, *Chem. Rev.*, 2017, **117**, 10121–10211.
110 L. Gao, K. Fan and X. Yan, *Nanozymology: Connecting Biology and Nanotechnology*, 2020, pp. 105–140.
111 L. Huang, K. Chen, W. Zhang, W. Zhu, X. Liu, J. Wang, R. Wang, N. Hu, Y. Suo and J. Wang, *Sens. Actuators, B*, 2018, **269**, 79–87.
112 J. M. Gonçalves, L. V. de Faria, A. B. Nascimento, R. L. Germscheidt, S. Patra, L. P. Hernández-Saravia, J. A. Bonacin, R. A. Munoz and L. Angnes, *Anal. Chim. Acta*, 2022, **1233**, 340362.
113 Q. Liu, S. Xin, X. Tan, Q. Yang and X. Hou, *Microchim. Acta*, 2023, **190**, 364.
114 M. K. Masud, J. Kim, M. M. Billah, K. Wood, M. J. Shiddiky, N.-T. Nguyen, R. K. Parsapur, Y. V. Kaneti, A. A. Alshehri and Y. G. Alghamidi, *J. Mater. Chem. B*, 2019, **7**, 5412–5422.

115 F. Tian, J. Zhou, B. Jiao and Y. He, *Nanoscale*, 2019, **11**, 9547–9555.
116 H. Zhu, Z. Quan, H. Hou, Y. Cai, W. Liu and Y. Liu, *Anal. Chim. Acta*, 2020, **1132**, 101–109.
117 L. Zhao, H. Guo, H. Chen, B. Zou, C. Yang, X. Zhang, Y. Gao, M. Sun and L. Wang, *Bioengineering*, 2022, **9**, 684.
118 H. kholafazad Kordasht, S. Hassanpour, B. Baradaran, R. Nosrati, M. Hashemzaei, A. Mokhtarzadeh and M. de la Guardia, *Biosens. Bioelectron.*, 2020, **165**, 112403.
119 O. D. Hendrickson, E. A. Zvereva, V. G. Panferov, O. N. Solopova, A. V. Zherdev, P. G. Sveshnikov and B. B. Dzantiev, *Biosensors*, 2022, **12**, 1137.
120 Y. Zhao, L. Li, R. Ma, L. Wang, X. Yan, X. Qi, S. Wang and X. Mao, *Anal. Chim. Acta*, 2021, **1173**, 338710.
121 X. Qi, L. Li, X. Yan, Y. Zhao, L. Wang, R. Ma, S. Wang and X. Mao, *J. Ocean Univ. China*, 2022, **21**, 1343–1350.
122 S. Wang, Y. Zhao, R. Ma, W. Wang, L. Zhang, J. Li, J. Sun and X. Mao, *Food Chem.*, 2023, **401**, 134053.
123 L. Li, R. Ma, Y. Zhao, L. Wang, S. Wang and X. Mao, *Talanta*, 2022, **246**, 123534.
124 F. Cui, Z. Zhou and H. S. Zhou, *Sensors*, 2020, **20**, 996.
125 J. Marfà, R. Pupin, M. Sotomayor and M. Pividori, *Anal. Bioanal. Chem.*, 2021, **413**, 6141–6157.
126 L. Wu, Y. Li, Y. Han, X. Liu, B. Han, H. Mao and Q. Chen, *J. Food Compos. Anal.*, 2024, **130**, 106190.
127 C. H. Cho, J. H. Kim, N. S. Padalkar, Y. V. M. Reddy, T. J. Park, J. Park and J. P. Park, *Biosens. Bioelectron.*, 2024, **255**, 116269.
128 C. Hernández-Cortez, I. Palma-Martínez, L. U. Gonzalez-Avila, A. Guerrero-Mandujano, R. C. Solís and G. Castro-Escarpulli, *Poisoning: from Specific Toxic Agents to Novel Rapid and Simplified Techniques for Analysis*, 2017, vol. 33.
129 R. Gupta, N. Raza, S. K. Bhardwaj, K. Vikrant, K.-H. Kim and N. Bhardwaj, *J. Hazard Mater.*, 2021, **401**, 123379.
130 K. Ren, M. Duan, T. Su, D. Ying, S. Wu, Z. Wang and N. Duan, *Talanta*, 2024, **270**, 125636.
131 H. Liang, H. Liu, H. Lin, G. Ning, X. Lu, S. Ma, F. Liu, H. Zhao and C. Li, *Food Sci. Hum. Wellness*, 2024, **13**, 2025–2035.
132 X. Cai, Y. Luo, C. Zhu, D. Huang and Y. Song, *Sens. Actuators, B*, 2022, **367**, 132066.
133 Y. Xing, F. Yasinjan, S. Sun, J. Yang, Y. Du, H. Zhang, Y. Liang, H. Geng, Y. Wang and J. Sun, *Nano Today*, 2024, **57**, 102386.
134 D. Li, T. Fan and X. Mei, *Nanoscale*, 2023, **15**, 15885–15905.
135 Q. Lu, Q. Li, Y. An, X. Duan, R. Zhao, D. Zhao and S. An, *J. Clean. Prod.*, 2022, **376**, 134117.
136 M. Tudi, H. Daniel Ruan, L. Wang, J. Lyu, R. Sadler, D. Connell, C. Chu and D. T. Phung, *Int. J. Environ. Res. Publ. Health*, 2021, **18**, 1112.
137 M. Song, *Improving Potable Reuse Water Quality by Understanding Bulk Organic Matter Present during Advanced Oxidation and N-nitrosodimethylamine Precursors*, University of Nevada, Reno, 2022.
138 N. K. V. Leitner, in *Advanced Oxidation Processes for Water Treatment: Fundamentals and Applications*, IWA Publishing, 2017, pp. 429–460.
139 Z. A. Mohamed, Y. Mostafa, S. Alamri, M. Hashem and S. Alrumman, *Arch. Microbiol.*, 2022, **205**, 63.
140 X. Yang, J. Pan, J. Hu, S. Zhao and K. Cheng, *Chem. Eng. J.*, 2023, **467**, 143381.
141 W. Jiang, Q. Yang, H. Duo, W. Wu and X. Hou, *Food Chem.*, 2024, **447**, 138917.
142 S. Zhang, H. Li, Q. Xia, D. Yang and Y. Yang, *J. Food Sci.*, 2024, **89**, 3618–3628.
143 R. Zhang, X. Yan and K. Fan, *Acc. Mater. Res.*, 2021, **2**, 534–547.
144 Y. Chong, Q. Liu and C. Ge, *Nano Today*, 2021, **37**, 101076.

